remote sensing

MDPI

Article

Change Detection Methods for Remote Sensing in the Last Decade: A Comprehensive Review

Guangliang Cheng [1,*,†], Yunmeng Huang [2,†], Xiangtai Li [3], Shuchang Lyu [2], Zhaoyang Xu [4], Hongbo Zhao [2], Qi Zhao [2] and Shiming Xiang [5]

[1] Department of Computer Science, University of Liverpool, Liverpool L69 3BX, UK
[2] Department of Electronic Information Engineering, Beihang University, Beijing 100191, China; lyushuchang@buaa.edu.cn (S.L.); bhzhb@buaa.edu.cn (H.Z.); zhaoqi@buaa.edu.cn (Q.Z.)
[3] School of Intelligence Science and Technology, Peking University, Beijing 100871, China
[4] Department of Paediatrics, Cambridge University, Cambridge CB2 1TN, UK; zx265@cam.ac.uk
[5] Institute of Automation, Chinese Academy of Sciences, Beijing 100190, China; smxiang@nlpr.ia.ac.cn
* Correspondence: guangliang.cheng@liverpool.ac.uk
† These authors contributed equally to this work.

Abstract: Change detection is an essential and widely utilized task in remote sensing that aims to detect and analyze changes occurring in the same geographical area over time, which has broad applications in urban development, agricultural surveys, and land cover monitoring. Detecting changes in remote sensing images is a complex challenge due to various factors, including variations in image quality, noise, registration errors, illumination changes, complex landscapes, and spatial heterogeneity. In recent years, deep learning has emerged as a powerful tool for feature extraction and addressing these challenges. Its versatility has resulted in its widespread adoption for numerous image-processing tasks. This paper presents a comprehensive survey of significant advancements in change detection for remote sensing images over the past decade. We first introduce some preliminary knowledge for the change detection task, such as problem definition, datasets, evaluation metrics, and transformer basics, as well as provide a detailed taxonomy of existing algorithms from three different perspectives: algorithm granularity, supervision modes, and frameworks in the methodology section. This survey enables readers to gain systematic knowledge of change detection tasks from various angles. We then summarize the state-of-the-art performance on several dominant change detection datasets, providing insights into the strengths and limitations of existing algorithms. Based on our survey, some future research directions for change detection in remote sensing are well identified. This survey paper sheds some light the topic for the community and will inspire further research efforts in the change detection task.

Keywords: change detection; remote sensing; algorithm granularity; supervision modes; comprehensive survey

Citation: Cheng, G.; Huang, Y.; Li, X.; Lyu, S.; Xu, Z.; Zhao, H.; Zhao, Q.; Xiang, S. Change Detection Methods for Remote Sensing in the Last Decade: A Comprehensive Review. *Remote Sens.* **2024**, *16*, 2355. https://doi.org/10.3390/rs16132355

Academic Editor: Carlos Alberto Silva

Received: 14 May 2024
Revised: 17 June 2024
Accepted: 24 June 2024
Published: 27 June 2024

1. Introduction

Change detection in remote sensing is the process of identifying changes in a scene from a pair of images captured in the same geographical area but at different time periods. With the rapid development of Earth observation technologies, acquiring large amounts of remote sensing images has become increasingly accessible. Consequently, change detection has emerged as a popular and fundamental task in the remote sensing community, with numerous real-world applications, such as urban development [1,2], agricultural surveys [3,4], land cover monitoring [5–7], disaster assessment [8], and military [9].

However, change detection poses some significant challenges [10–12], as paired images are often captured under varying conditions, such as different angles, different illuminations, and even different seasons, resulting in diverse and unknown changes in a scene.

These challenges encompass a broad range of issues, including (1) variations in image quality arising from differences in spatial, spectral, and temporal resolutions; (2) the presence of diverse types of noise and artifacts; (3) errors during image registration; (4) difficulties in handling illumination, shadows, and changes in viewing angle; (5) complex and dynamic landscapes; and (6) scale and spatial heterogeneity of the landscape.

Over the past few decades, numerous change detection methods have been proposed. Before the deep learning era, pointwise classification methods [3,13–22] witnessed great progress in change detection tasks. Most traditional methods focus on detecting the changed pixels and classifying them to generate a change map. A variety of machine learning models have been applied to the change detection task, including support vector machines (SVMs) [13,14], random forests [15], decision trees [16], level sets [17,18], Markov random fields (MRFs) [3,22], and conditional random fields (CRFs) [19–21]. Though some specific images can achieve considerable performance with the above methods, they still suffer from low accuracy and lack of generalization ability. Moreover, their performance is highly dependent on the decision classifiers and threshold settings.

In recent years, the rapid development of deep learning technologies [23,24], particularly deep convolutional neural networks (CNNs), has led to the emergence of CNN models that have shown superior performance over traditional methods for change detection tasks, as evidenced by numerous studies [9,25–32]. This is mainly attributed to the exceptional representation and nonlinear characterization capabilities of CNNs, which make them a more effective choice for obtaining optimal performance in this field.

Recently, attention models [33–38] have been proposed to capture spatial and temporal dependencies within image pairs for change detection tasks. These models leverage an attention mechanism to focus on crucial areas, enabling them to better identify subtle changes in the scene and distinguish them from usual scene variability. On the other hand, transformer models [4,39–46] employ a self-attention mechanism to learn global relationships between the image pixels, allowing them to capture long-term dependencies and spatial correlations. They have shown promising results in tasks that require modeling temporal sequences, such as video processing [47] and language translation [48]. Both attention models and transformer models have shown significant improvements over traditional methods and vanilla CNNs in change detection tasks, making them promising avenues for further research and development in the field of remote sensing.

With the plethora of recent change detection methods that rely on deep learning strategies, many works have emerged to survey these methods. Some of these works consider deep learning methods in general [10–12,49–52]; while others focus on specific aspects, such as multisource remote sensing images and multiobjective scenarios [49], high-resolution remote sensing images [11], 3D point cloud data [51], multiscale attention methods [52], etc. Moreover, it is worth noting that the most recent survey method only accounts for algorithms up to 2021. Figure 1 depicts the statistical analysis of published papers related to the change detection algorithms over the past decade, as recorded in the DBLP https://dblp.org/ (accessed on 10 May 2024). Based on the findings, we can conclude that the topic will be further explored with deep learning, and an increasing number of research works will be published in the forthcoming years. However, in light of the increased focus on attention and transformer methods [47,53,54], diffusion methods [55,56], and Mamba architectures [57–59] in recent years, there has been a notable proliferation of proposed change detection tasks. Thus, it is imperative to conduct a comprehensive change detection survey that encompasses the latest state-of-the-art methodologies.

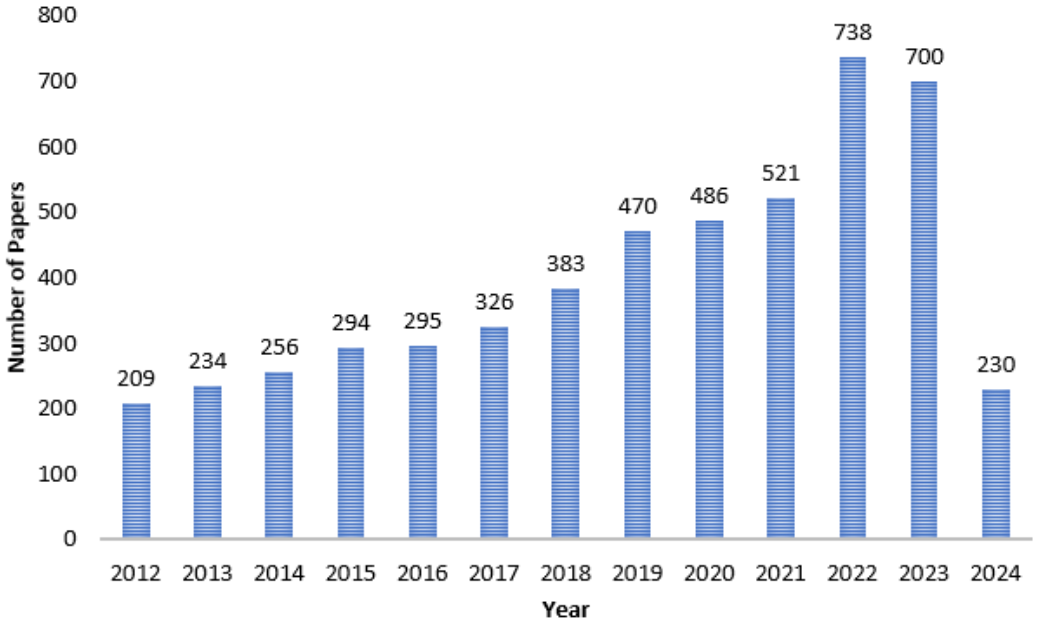

Figure 1. Statistics on the literature of change detection in the past decade.

In summary, this survey has three main contributions:

- Compared to the previous survey works on change detection [10–12,49–52,60–62], our study provides a more comprehensive overview of the latest research on change detection in the past decade. Moreover, we systematically review the entirety of current algorithms to date and offer a relatively comprehensive depiction of the current state of the field.
- Several systematical taxonomies of current change detection algorithms are presented from three perspectives: algorithm granularity, supervision modes, and learning frameworks. Furthermore, some influential works published with state-of-the-art performance on several dominant benchmarks are provided for future research.
- Change detection learning schemes and their applications remain a rapidly developing research field, as illustrated in Figure 1, and many challenges need to be addressed. In this paper, we comprehensively review the existing challenges in this field and provide our perspective on future trends.

Scope: This survey aims to cover the mainstream change detection algorithms from three perspectives, algorithm granularity, supervision modes, and learning frameworks, as depicted in Figure 2. The algorithms within the three taxonomies are carefully selected to ensure their orthogonality, thereby complementing each other and maintaining their distinctiveness. This survey focuses on the most representative works, despite the abundance of preprints or published works available. Additionally, we benchmark several predominant datasets and provide a detailed discussion of future research trends.

Organization: This paper is organized as follows. In Section 2, we review the preliminary knowledge of change detection, i.e., task definition, dominant datasets, evaluation metrics, and some transformer basics. In Section 3, we take a closer look at existing methods and classify them from three perspectives. Section 4 benchmarks the state-of-the-art performance on several popular change detection datasets. Section 5 raises future research trends and discussions. Finally, we conclude this survey in Section 6.

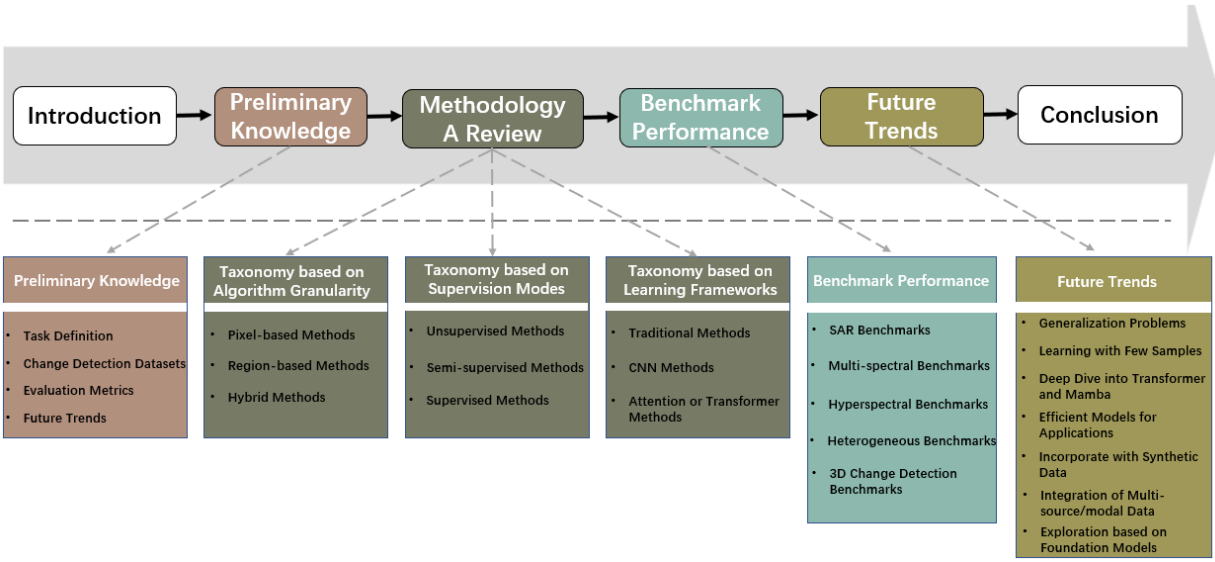

Figure 2. Illustration of the pipeline of this survey. Different colors represent specific sections. Best viewed in color.

2. Preliminary Knowledge

In this section, we first introduce the task of change detection in remote sensing and provide a comprehensive definition. Subsequently, we delve into various popular change detection datasets from diverse data sources and present some crucial evaluation metrics that are utilized in the benchmark part to assess the performance of different methods. Finally, we introduce some basic knowledge of transformers that are extensively utilized in modern attention- and transformer-based algorithms.

2.1. Task Definition

Change detection in remote sensing refers to the process of identifying and quantifying changes in the land surface over time using remotely sensed data. It can be formally defined as follows: As Figure 3 shows, given two or more remotely sensed images of the same area captured at different times, the change detection task aims to identify changes in the land surface, such as changes in land cover or land use, natural phenomena, or human activities, by comparing the pixel values of the images and applying appropriate change detection algorithms. According to the position of the fusion module, existing change detection algorithms, especially the deep learning methods, can be categorized into three groups: early-fusion methods (Figure 3a), middle-fusion methods (Figure 3b), and late-fusion methods (Figure 3c). For the fusion methods, element-wise subtraction [63,64], element-wise concatenation [65,66], and majority voting [67] are widely used.

Moreover, the whole pipeline of the change detection task can be divided into several subtasks, including the following:

- **Image preprocessing**: This involves removing noise, correcting geometric and radiometric distortions, and enhancing image quality to ensure the images are properly aligned and suitable for analysis.
- **Image registration**: This involves aligning the images spatially and temporally to ensure that corresponding pixels in each image are accurately compared.
- **Change detection algorithm selection**: To accurately detect changes in images, it is crucial to select the appropriate change detection algorithms based on the application and image characteristics. This can include traditional methods as well as more advanced techniques such as CNN methods or transformer methods.
- **Postprocessing**: This involves removing noise and false positives and generating a final change map that accurately represents the changes. It is worth noting that this step is not mandatory and can be skipped.

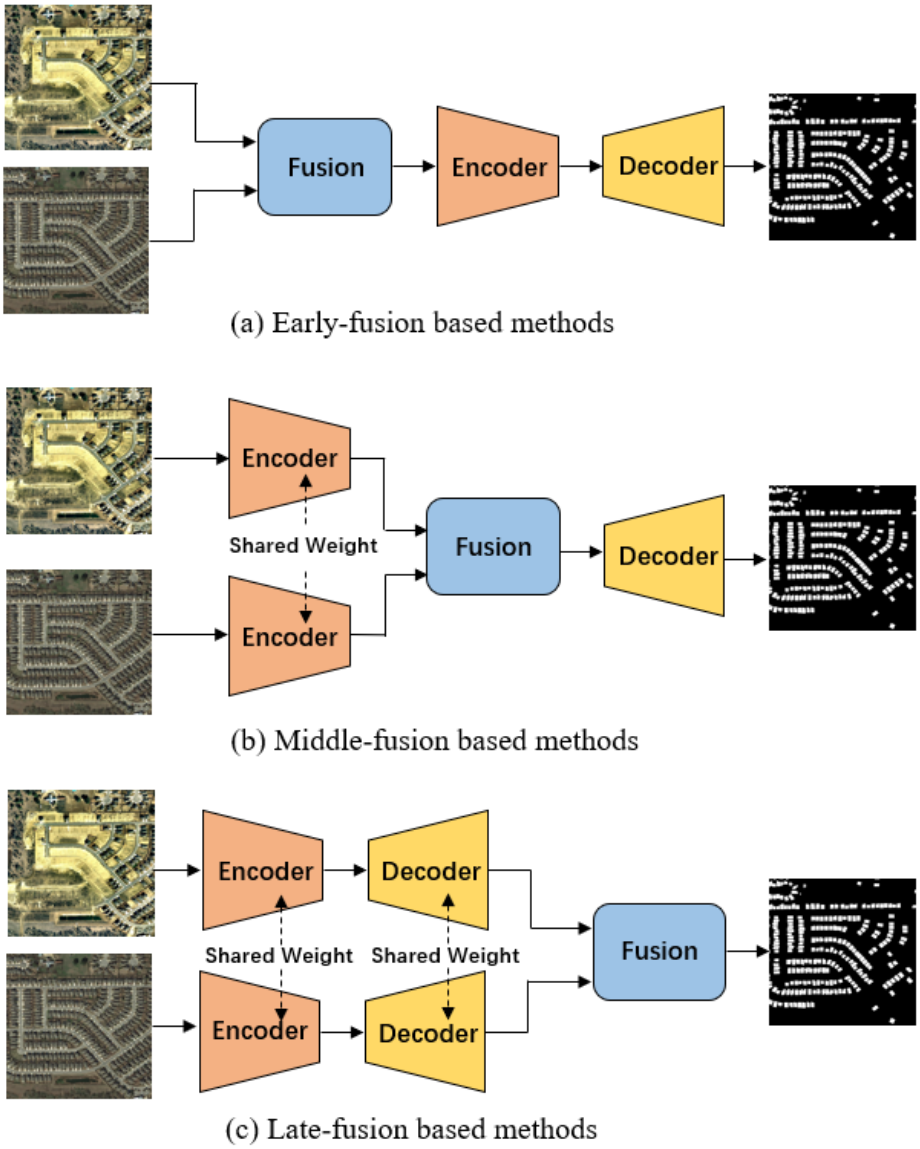

Figure 3. The existing frameworks for the change detection task. They can be classified into three categories based on the position of the fusion module, including early-fusion methods, middle-fusion methods, and late-fusion methods. Please note that this criterion is not limited to the deep learning methods; it also encompasses traditional methods.

In this paper, our focus lies primarily on the change detection algorithms. For a comprehensive understanding of the other steps involved, readers are recommended to refer to existing works [50,61,68].

As shown in Figure 3, given two input data pairs, $\mathbf{D}_1 \in \mathcal{R}^{P\times N}$ and $\mathbf{D}_2 \in \mathcal{R}^{P\times M}$, captured at the same location at different times. For images, P denotes $H \times W$ for the images with width W and height H. For point cloud data, P represents the number of points. Specifically, the change detection algorithms can be summarized as follows:

$$\mathbf{M} = CD(PR(\mathbf{D}_1), PR(\mathbf{D}_2)), \tag{1}$$

where PR denotes the image **p**reprocessing and **r**egistration steps to ensure that the paired images are well aligned. CD denotes the change detection algorithm. The output maps of the changed area are represented by $\mathbf{M}$. According to the different input data sources, both $\mathbf{D}_1$ and $\mathbf{D}_2$ can come from homogeneous data sources, such as synthetic aperture radar (SAR) images, multispectral images (including the optical images), hyperspectral images,

and point cloud data. $\mathbf{D}_1$ and $\mathbf{D}_2$ can also originate from different data sources, which are referred to as "heterogeneous data". Based on different types of output, change detection tasks can be classified into two categories: binary change detection [69,70], which differentiates between changed and unchanged areas, and semantic change detection [71–73], which identifies changes in the categories or labels of objects before and after the change.

2.2. Change Detection Datasets

In the following, we summarize some dominant change detection datasets from the past few decades. To facilitate correspondence with various methods, the datasets are presented in five distinct categories based on the type of data sources, i.e., SAR data, multispectral data, hyperspectral data, heterogeneous data, and 3D change detection data. For more details about the change detection datasets, readers can refer to the project websites https://github.com/wenhwu/awesome-remote-sensing-change-detection (accessed on 15 April 2024); https://github.com/yjt2018/awesome-remote-sensing-change-detection (accessed on 15 April 2024).

SAR data: Synthetic aperture radar (SAR), as a special type of radar, utilizes electromagnetic signals to generate two-dimensional or three-dimensional images of objects. These images can be applied for multiple purposes, such as object detection in and geographical localization and geophysical property estimation of complex environments. SAR has the advantage of working in all weather conditions, penetrating through vegetation and clouds, and has high-resolution imaging capabilities to identify small features, making it suitable for remote sensing analysis. However, SAR systems can be susceptible to geometric distortion, electromagnetic interference, and speckle noise, which need to be addressed in industrial applications (shown in the first block of Table 1). For the SAR datasets, we present two dominant datasets, i.e., Yellow River [74] and Bern [75], along with their specific details shown in Table 2. Specifically, Yellow River [74] consists of two SAR images of the Yellow River Estuary in China, each with dimensions of 7666 $\times$ 7692 pixels. These images were captured by the Radarsat-2 satellite in June 2008 and June 2009, respectively, and are commonly utilized for studying changes in this region, making it a valuable resource for various change detection methods applied to the SAR images. Bern [75] comprises two SAR images, each with dimensions of 301 $\times$ 301 pixels, covering the city of Bern, Switzerland. The images were acquired by the European Remote Sensing Satellite-2 (ERS-2) in April and May of 1999. Notably, the May 1999 image captured the impact of flooding caused by the Aare River on the airport in Bern City.

Table 1. The summary of advantages and disadvantages for different data sources in the remote sensing change detection task.

	Advantages	Disadvantages
SAR data	(1) Can penetrate through vegetation and clouds; (2) Can detect subtle changes in object scattering; (3) Can provide information on surface deformation; (4) Can work well in all weather conditions.	(1) Can be susceptible to geometric distortion; (2) Can be subject to electromagnetic interference; (3) Can be complex and difficult to interpret; (4) SAR sensors are expensive to develop and maintain.
Multispectral data	(1) Can distinguish materials based on spectral information; (2) Multispectral sensors are relatively inexpensive; (3) Multispectral images are widely available.	(1) Multispectral sensors have limited spectral resolution; (2) Images are susceptible to atmospheric interference; (3) Images are affected by land cover and seasonal changes.
Hyperspectral data	(1) Can distinguish materials with similar spectral signatures; (2) Can provide rich information about the chemical and physical properties of materials.	(1) Hyperspectral sensors are relatively expensive; (2) Hyperspectral sensors may have limited spatial resolution; (3) Images are susceptible to atmospheric interference.
Heterogeneous data	(1) Heterogeneous images can provide complementary information and improve the overall accuracy and quality of the output by combining data from different sensors.	(1) The integration of heterogeneous images can be complex and challenging; poor quality or mismatched data can lead to artifacts, noise, or errors in the fusion process.
Three-dimensional change detection data	(1) Can capture fine details and subtle changes; (2) Can penetrate through dense vegetation and provide accurate elevation information.	(1) Collection and processing are costly and time-consuming; (2) The accuracy and quality of the output depend on the quality of the calibration and the presence of noise.

Table 2. The detailed information of several dominant change detection datasets. Note that the quantity of data is represented by the number of data pairs.

Dataset	Resolution	Quantity	Location	Types	Date	Category
SAR Dataset						
Yellow River [74]	7666 × 7692	1	Yellow River Estuary, China	Radarsat-2	June 2008 June 2009	2
Bern [75]	301 × 301	1	Bern, Switzerland	European Remote Sensing Satellite-2	April 1999 May 1999	2
Multispectral Dataset						
LEVIR-CD+ [76]	1024 × 1024 0.5 m/pixel	985	American cities	Google Earth	2002 to 2018	2
CDD [77]	4725 × 2700 1900 × 1000 0.03–1 m/pixel	7 4	–	Google Earth	–	2
WHU-CD [78]	21,243 × 15,354 11,265 × 15,354 0.3 m/pixel	1 1	Christchurch, New Zealand	–	–	2
SECOND [79]	512 × 512 0.5–3 m/pixel	4662	Hangzhou, Chengdu, Shanghai, China	–	–	6
SYSU-CD [80]	256 × 256 0.5 m/pixel	20,000	Hong Kong	–	2007 to 2014	5
Hyperspectral Dataset						
River [81]	463 × 241	1	Jiangsu, China	EO-1 sensor	3 May 2013 21 December 2013	2
Hermiston [82]	307 × 241	1	Hermiston City, USA	Hyperion sensor	1 May 2004 8 May 2007	2
Farmland [83]	450 × 140	1	Yancheng, China	EO-1 sensor	3 May 2006 23 April 2007	2
Heterogeneous Dataset						
California [84]	850 × 500	2	California, USA	Landsat-8 Sentinel-1A	5 January 2017 18 February 2017	2
3D Change Detection Dataset						
3DCD [85]	400 × 400 0.5 m/pixel 200 × 200 1 m/pixel	472 2D 472 3D	Valladolid, Spain	–	2010 2017	2

Multispectral data: Multispectral images can be used to identify and map various features on the Earth's surface, such as vegetation, water bodies, and urban areas. Each type of feature reflects or emits energy uniquely, and the information captured by the different spectral bands can be used to distinguish between them. For example, healthy vegetation typically reflects more energy in the near-infrared part of the spectrum than other types of land cover, which makes it possible to identify and map areas of vegetation using multispectral data. The advantages and disadvantages of multispectral images are detailed in the second block of Table 1. Four primary multispectral datasets, i.e., LEVIR-CD+ [76], CDD [77], WHU-CD [78], SECOND [79], and SYSU-CD [80], are introduced. Specifically, LEVIR-CD+ is a comprehensive remote sensing change detection resource, containing 985 pairs of very-high-resolution (VHR, 0.5 m/pixel) Google Earth images, each measuring 1024 × 1024 pixels. The dataset, as described by Chen et al. [76], centers on detecting building changes in American cities between 2002 and 2018, with a particular focus on building growth and decline. CDD [77], also referred to as the season-varying dataset, is a collection of VHR (i.e., 0.03–1 m/pixel) images comprising seven pairs of images with dimensions of 4725 × 2700 pixels and four pairs with dimensions of 1900 × 1000 pixels. The dataset, sourced from Google Earth, focuses on capturing seasonal variations in natural objects of varying sizes. The WHU-CD [78] dataset is one subset from the larger WHU Building dataset, tailored for the building CD task. The aerial imagery dataset covers the city of Christchurch, New Zealand, and contains images with a ground resolution of 0.3 m. The dataset is composed of a pair of images with a resolution of 32,508 × 15,354 pixels, capturing an area both before and after a 6.3-magnitude earthquake. According to the official protocol, it is split into a training (21,243 × 15,354) area and a testing (11,265 × 15,354) area. This dataset is particularly useful for researchers interested in building damage detection and assessment after natural disasters, as well as for those interested in developing ma-

chine learning algorithms for automated building change detection. SECOND [79], as a semantic change detection dataset, is composed of 4662 pairs of aerial images obtained by several platforms and sensors. The dataset covers cities such as Hangzhou, Chengdu, and Shanghai, and each image pair has the same dimensions of 512 × 512 pixels, with a spatial resolution varying from 0.5 to 3 m/pixel. This dataset is particularly useful for researchers interested in studying human-made geographical and natural changes, covering six main categories. For the change category, the SECOND dataset focuses on six main land cover classes, i.e., nonvegetated ground surface, trees, low vegetation, water, buildings, and playgrounds. SYSU-CD [80] presents a category-agnostic CD dataset, comprising a set of 20,000 pairs of 0.5 m/pixel resolution aerial images from Hong Kong, spanning 2007 to 2014. It encompasses a range of various change scenarios such as urban construction, suburban expansion, groundwork, vegetation changes, road expansion, and sea construction.

Hyperspectral data: Hyperspectral imaging [86] is a technique that captures and analyzes numerous narrow, contiguous spectral bands across the electromagnetic spectrum. Unlike multispectral images, which typically capture data in a few broad spectral bands, hyperspectral images capture data across hundreds of spectral bands, providing highly detailed information about the composition and characteristics of the image materials. The high spectral resolution of hyperspectral images enables the identification and discrimination of materials that may have similar appearances but different spectral signatures, such as different types of vegetation or minerals. Hyperspectral imaging is widely used in remote sensing applications, such as environmental monitoring, mineral exploration, and crop health assessment. The advantages and disadvantages of hyperspectral images are detailed in the third block of Table 1. For the hyperspectral data, River [81], Hermiston [82] and Farmland [83] are utilized in this survey. The details of these datasets can be found in Table 2. River [81] comprises two hyperspectral images (HSI) sized 463 × 241 pixels. The images were captured on 3 May and 21 December 2013, respectively, and primarily cover a river in Jiangsu Province. Hermiston [82], encompassing an agricultural area in Hermiston City, was obtained by a Hyperion sensor. The dataset contains a pair of HSIs collected on 1 May 2004, and 8 May 2007, respectively. The images have a resolution of 307 × 241 pixels and comprise a selection of 154 bands from a total of 242 spectral bands. Farmland [83] consists of two HSIs acquired by Earth Observing-1 (EO-1) on 3 May 2006, and 23 April 2007, respectively. The dataset covers farmland near Yancheng, Jiangsu Province, and has 155 bands for experiments after removing the low-noise spectral bands. The spatial size is 450 × 140 pixels. The main changes in the dataset were caused by the cultivation of crops.

Heterogeneous data. The term "heterogeneous data" in remote sensing refers to images that combine data from multiple sources or sensors with different characteristics, such as SAR images, multispectral images, hyperspectral images, and LiDAR data. By integrating data from different sources, heterogeneous images can provide more comprehensive and accurate information about the Earth's surface than individual sensor data alone. For example, combining optical and SAR data can enable better identification and characterization of land cover types, while integrating LiDAR data can provide information about the three-dimensional structure of vegetation and terrain. Heterogeneous image analysis techniques have become increasingly important in remote sensing applications such as land use and land cover mapping, environmental monitoring, and disaster management. However, the integration and processing of data from multiple sources also pose significant challenges, including data registration, normalization, and fusion. The advantages and disadvantages of heterogeneous images are summarized in the fourth block of Table 1. In this survey, we introduce the California dataset [84], which includes both SAR images and multispectral images. A summary of this dataset is provided in Table 2. The California dataset [84] contains one multispectral image and two SAR images. The multispectral image was collected on 5 January 2017 by Landsat-8. Most bands in it have a resolution of 30 m. The SAR images were captured on February 18, 2017 by Sentinel-1A. The dataset covers the same region in Sacramento County, Yuba County, and Sutter County, California, where flooding has caused the changes.

Three-dimensional change detection data: 3D point cloud data refers to a collection of points in three-dimensional space that represent the surface of an object or a terrain. In remote sensing, 3D point cloud data are obtained by using light detection and ranging (LiDAR) technology, which uses laser pulses to measure the distance between the sensor and the ground or other objects. For change detection applications, 3D change detection data can be used to identify differences in terrain or object heights and shapes over time. This is particularly useful for monitoring natural and human-made features such as buildings, vegetation, and coastlines. The advantages and disadvantages of 3D change detection data are summarized in the final row of Table 1. For the 3D change detection dataset, 3DCD [85] is employed to benchmark the state-of-the-art performance in this survey. 3DCD [85] comprises a total of 472 image pairs, each consisting of optical orthophotos cropped to the same size, along with the corresponding 2D change detection maps in raster format. The images were obtained by two aerial surveys in 2010 and 2017 separately. A total of 472 pairs of digital surface models (DSMs) produced from the rasterization of point clouds and the corresponding 3D change detection maps are also included in the dataset. The 2D change detection maps have a resolution of 0.5 m with a size of 400 × 400 pixels, while the 3D change detection maps have a resolution of 1 m with a size of 200 × 200 pixels. The dataset focuses on the urban area of Valladolid, Spain.

2.3. Evaluation Metrics

Evaluation metrics are essential in evaluating the performance of a change detection model. This study presents a concise introduction and analysis of common evaluation metrics. These include true positive (TP) and true negative (TN), which indicate the number of correctly identified changed and unchanged pixels, respectively. On the other hand, false positives (FP) and false negatives (FN) refer to the number of pixels wrongly classified as changed or unchanged, respectively. A high precision value implies the algorithm's ability to identify changed pixels accurately. In contrast, a high recall value suggests the algorithm can detect a higher proportion of changed pixels from the ground-truth data. The intersection over union (IoU) represents the ratio of intersection and concatenation of the predicted map and ground truth. The overall accuracy (OA) metric indicates the prediction's accuracy. The F1 score is a harmonic average of precision and recall. Additionally, other metrics are designed for specific applications, such as the kappa coefficient (KC) [87], which measures classification accuracy based on the confusion matrix. RMSE (root mean squared error) and cRMSE (changed root mean squared error) [88] are commonly used for evaluating 3D change detection model change detection performance. cRMSE considers only errors in ground-truth pixels influenced by altitude. In semantic change detection (SCD), mean intersection over union (mIoU), separated kappa (Sek), and SCD-targeted F1 score (F_{scd}) are used to evaluate accuracy.

$$\mathrm{IoU} = \frac{\mathrm{TP}}{\mathrm{TP} + \mathrm{FN} + \mathrm{FP}}\ , \tag{2}$$

$$\mathrm{OA} = \frac{\mathrm{TP} + \mathrm{TN}}{\mathrm{TP} + \mathrm{FP} + \mathrm{TN} + \mathrm{FN}}\ , \tag{3}$$

$$\mathrm{F_1} = \frac{2\mathrm{TP}}{2\mathrm{TP} + \mathrm{FP} + \mathrm{FN}}\ , \tag{4}$$

$$\mathrm{RMSE} = \sqrt{\frac{1}{n}\sum_{i=1}^{n}(\widehat{\Delta H_i} - \Delta H_i)^2}\ , \tag{5}$$

$$\mathrm{cRMSE} = \sqrt{\frac{1}{n_c}\sum_{i=1}^{n_c}(\widehat{\Delta H_i}^{C} - \Delta H_i^{C})^2}\ . \tag{6}$$

For more information about these metrics, readers can refer to [72].

2.4. Transformer Basics

Attention basics: Attention [33] algorithms are a type of machine learning algorithm that selectively focus on certain aspects of data or inputs while ignoring others. They assign different weights or importance values to different parts of the input based on their relevance to the task at hand. Attention algorithms have become increasingly popular in natural language processing (NLP) [89] and computer vision applications [90], as they enable models to focus on the most relevant information in a sentence or image. As depicted in Figure 4a, given the key (K), query (Q), and value (V), the attention mechanism can be defined as

$$\mathrm{Att}(Q, K, V) = \mathrm{Softmax}(\frac{QK^T}{\sqrt{d_k}})V. \tag{7}$$

The scale factor d_k represents the dimension of the keys in the attention mechanism. The resulting attention map is multiplied with V to focus on the most relevant regions. In practice, a multihead attention (MHA) module with h heads is often used instead of a single attention function shown in Equation (7). As shown in Figure 4b, the MHA involves performing multiple attention operations in parallel and concatenating the attention results as

$$\mathrm{MHA}(Q, K, V) = W_P\mathrm{Concat}([Att_1, Att_2, ..., Att_h]). \tag{8}$$

where the information from different heads is concatenated, then the concatenated outputs are fused together using a projection matrix W_P, which allows the model to effectively incorporate information from multiple heads of attention. Based on the different sources of query (Q) and key (K), MHA can be divided into multihead self-attention (MHSA) and multihead cross-attention (MHCA). MHSA refers to the case where the Q and K for all heads come from the same sequences or tokens, while MHCA refers to the case where Q and K for different heads come from different sequences or tokens.

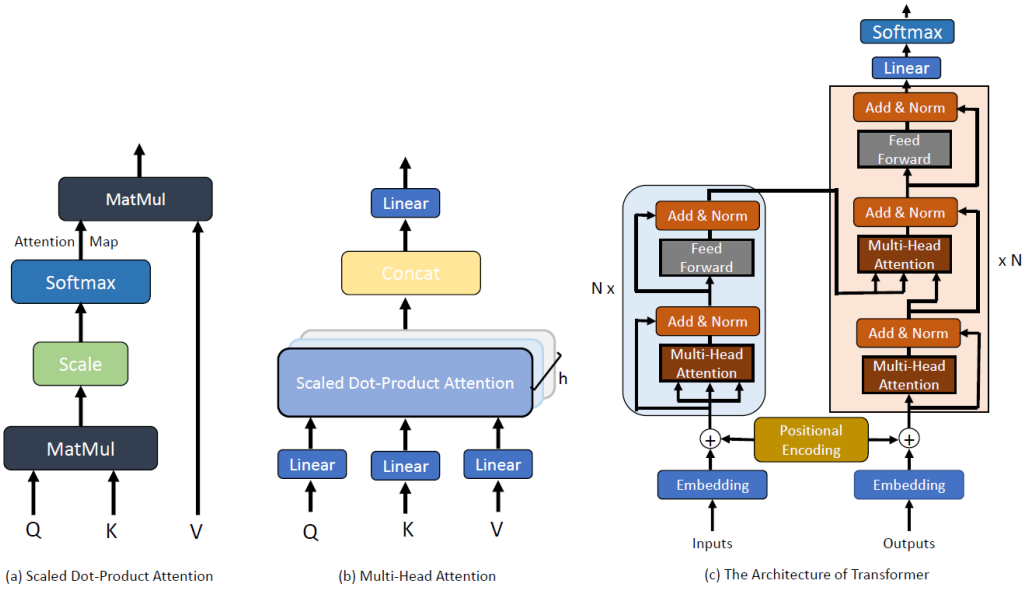

Figure 4. Some preliminary knowledge of the transformer.

Transformer basics: As shown in Figure 4c, the transformer architecture [54] comprises an encoder and a decoder, both of which contain multiple layers of multihead attention (MHA) and feedforward neural networks (FFNs). In particular, the FFN consists of two consecutive multilayer perceptrons (MLPs) with a nonlinear activation function. In addition to the MHSA, the decoder utilizes MHCA to attend to the relevant information or regions from different multimodal sequences. Unlike the CNNs and attention mechanism, the transformer adds positional encoding information to input and output embedding to capture positional information.

3. Methodology: A Survey

In this section, we comprehensively review methodologies from three distinct perspectives: (1) taxonomy based on algorithm granularity, (2) taxonomy based on supervision modes, and (3) taxonomy based on learning frameworks. It is imperative to note that the presented algorithms from these three taxonomies are carefully chosen to ensure orthogonality, thereby complementing one another. Furthermore, given the discrepancies in data quantities and unique data characteristics across various data sources, we present a comprehensive introduction to the existing approaches categorized by data type in the following.

3.1. Taxonomy Based on Algorithm Granularity

As introduced in the previous section, the remote sensing community categorizes data for the change detection task based on the types of available data sources. For each data source, we classify the change detection methods based on the algorithm granularity into the following categories: pixel-based methods, region-based methods, and hybrid methods:

- **Pixel-based methods:** Pixel-based methods are commonly used for image segmentation tasks [91–94] in computer vision. These methods assign a label to each individual pixel in an image based on its spectral characteristics, with the goal of partitioning the image into regions of different classes. Traditional pixel-based methods often suffer from false positives and false negatives. Fortunately, with the advent of deep learning and its increased receptive field, such as the pyramid pooling module [95], atrous convolution [96], and attention module [33], pixel classification methods based on deep learning can achieve significantly improved performance. It is worth noting that most end-to-end CNN models fall under the category of pixel-based methods.
- **Region-based methods:** Region-based methods [97,98], also known as object-based methods, leverage image segmentation techniques first to group pixels into meaningful regions, such as objects, superpixels, or bounding boxes, based on their spatial, spectral, and contextual characteristics. These grouped regions are then used as the units for detecting and recognizing the changed results with either traditional or deep learning methods.
- **Hybrid methods:** The use of hybrid methods [19,38,99] has been identified as a powerful approach for change detection tasks. These methods leverage the advantages of multiple individual techniques such as pixel-based methods, region-based methods, or a combination of both to achieve improved accuracy in change detection. By integrating different methodologies, hybrid approaches can address the limitations of each method and provide a more robust and comprehensive solution for detecting changes in remote sensing imagery. These methods typically involve the parallel or successive use of pixel-based and region-based techniques to detect changes from different perspectives.

In the following, we present an overview of change detection algorithms based on algorithm granularity for each available data source.

(1) SAR methods. The first block in Table 3 presents some representative literature for SAR change detection algorithms. Among the pixel-based methods, Atasever et al. [100] propose an unsupervised change detection approach based on arc-tangential difference, Gaussian and median filters, and K-means++ clustering. JR-KSVD [101] introduces a joint-related dictionary learning algorithm based on the k-singular value decomposition and an iterative adaptive threshold optimization algorithm for unsupervised change detection. Vinholi et al. [102] present an incoherent change detection algorithm based on CNNs, which includes a segmentation CNN to localize potential changes and a classification CNN to further analyze the potential changes to classify them as real changes or false alarms. Among the region-based methods, Yang et al. [97] propose a region-based change detection method that first utilizes the customized simple linear iterative clustering algorithm [103] to generate superpixels and then employs Wishart mixture models to model each local

superpixel. Amitrano et al. [104] exploit multitemporal geographical object-based image analysis, which involves classifying the data using a dictionary representation approach and combining class-specific information layers through fuzzy logic to bring out the underlying meaning in the data. For the hybrid methods, UAFS-HCD [105] proposes a new unsupervised fusion method for change detection, which employs an intuitive decision-level fusion scheme of pixel-based method and region-based method. Javed et al. [106] propose a new approach for detecting recently developed urban areas by utilizing the Dempster–Shafer theory to extend the results of the pixel-based method into a region-based method.

Table 3. The representative literature on various algorithms' granularity for different data sources in change detection tasks. We also illustrate the fusion category for each approach.

Method	Source	Category	Fusion	Highlights
SAR Methods				
ARCT+ [100]	GRSL 2022	Pixel-based	Middle	The arc-tangential subtraction operator is applied to obtain a difference image, which is then subjected to K-means++ clustering to identify the changed regions.
JR-KSVD [101]	J-STARS 2022	Pixel-based	Late	Proposes a joint-related dictionary learning algorithm based on K-SVD and an iterative adaptive threshold optimization.
Incoherent CDA [102]	GRSL 2022	Pixel-based	Early	Utilizes a segmentation CNN to localize potential changes and a classification CNN to further inspect potential changes as true changes or false alarms.
WMMs [97]	TGRS 2016	Region-based	Middle	Segments the PolSAR images into compact local regions, and then wishart mixture models (WMMs) are used to model each local region.
OBIA [104]	TGRS 2022	Region-based	Middle	Takes advantages of consolidated SAR techniques and modern geographical object-based image analysis (GEOBIA).
UAFS-HCD [105]	J-STARS 2015	Hybrid	Late	Obtains the preliminary change mask with pixel-based change detection method and obtains the final change mask using the object-based change detection method.
DSF [106]	Remote Sensing 2020	Hybrid	Middle	Detects the change detection results by extending pixel-based object detection method into an OBCD through the Dempster–Shafer theory.
Multispectral Methods				
ADHR-CDNet [107]	TGRS 2022	Pixel-based	Early	Proposes an HRNet with differential pyramid module, and a multiscale spatial feature attention module is presented to fuse different information.
LWCDNet [108]	GRSL 2022	Pixel-based	Early	Proposes a lightweight fully convolution network with convolutional block attention module and Lov-wce loss.
COCRF [5]	TGRS 2022	Region-based	Early	Proposes a class-prior object-oriented conditional random field framework to handle binary and multiclass change detection tasks.
SSS-CD [109]	Remote Sensing 2022	Region-based	Early	Integrates spectral–spatial–saliency change information and fuzzy integral decision fusion for the change detection task.
DP-CD-Net [110]	GRSL 2022	Hybrid	Early	Proposes a dual-pathway feature difference network, an adaptive fusion module, and an auxiliary supervision strategy.
Hyperspectral Methods				
GETNET [81]	TGRS 2019	Pixel-based	Early	Proposes a general end-to-end 2D CNN for hyperspectral image change detection.
SSA-SiamNet [111]	TGRS 2022	Pixel-based	Middle	Proposes an end-to-end Siamese CNN with a spectral–spatial-wise attention mechanism.
CDFormer [45]	GRSL 2022	Pixel-based	Middle	Introduces a transformer encoder to the hyperspectral image change detection framework.
FuzCVA [112]	IGARSS 2018	Hybrid	Middle	Proposes a fuzzy inference combination strategy that combines the angle and magnitude distances.
MSDFFN [83]	TGRS 2023	Hybrid	Middle	Proposes bidirectional diff-changed feature representation module and a multiscale attention fusion module to fuse the changed features.
Heterogeneous Methods				
SCCN [27]	TNNLS 2018	Pixel-based	Middle	Proposes a symmetric convolutional coupling network for unsupervised change detection tasks.
SSPCN [113]	J-STARS 2021	Pixel-based	Middle	Introduces a classification method to obtain the pseudo labels and then a spatially self-paced convolutional network to update the pseudo-label labels to obtain better results.
MSGCN [114]	IJAEOG 2022	Region-based	Middle	Introduces a new change detection method based on the graph convolutional network and multiscale object techniques.
CMS-HCC [115]	TGRS 2019	Region-based	Middle	Proposes a region-based change detection method with a cooperative multitemporal segmentation process and a hierarchical compound classification process.
HMCNet [38]	TGRS 2022	Hybrid	Middle	Proposes an MLP-CNN hybrid model with multilayer perceptron and convolutional neural network to achieve change detection result.
CD-GAN [116]	Arxiv 2022	Hybrid	Middle	Introduces a robust fusion-based adversarial framework that fuses the results from predefined and previously trained networks.
Three-Dimensional Change Detection Methods				
HDG-nDSM [117]	Remote Sensing 2023	Pixel-based	Middle	Proposes a height difference-generated nDSM, including morphological filters and criteria considering area size and shape parameters.
DALE-CD [118]	ISPRS Archives 2022	Pixel-based	Early	Proposes a 3D change detection method based on density-adaptive local Euclidean distance.
CHM-CD [119]	TGRS 2018	Region-based	Middle	First detects the large changes and then focuses on the individual tree canopy to detect the single-tree changes by means of an object-based CD.

(2) Multispectral methods. The second block of Table 3 showcases a collection of the representative literature on methods for change detection in multispectral images. Among the pixel-based methods, ADHR-CDNet [107] proposes an attentive differential high-resolution change detection network, which introduces a new high-resolution backbone with a differential pyramid module. Bu et al. [120] propose a new deep learning framework for change detection tasks, which consists of two collaborative modules to improve the estimation accuracy and computation efficiency. LWCDNet [108] proposes a lightweight convolution network for change detection with a typical encoder–decoder structure, an artificial padding convolution module, and a convolutional block attention module. For the region-based methods, Shi et al. [5] introduce a class-prior object-oriented conditional random field framework, which consists of a binary change detection task and a multiclass change detection task. Ge et al. [109] propose an object-oriented change detection approach that integrates spectral–spatial-saliency change information and fuzzy integral decision fusion to eliminate the detection noise. Among the hybrid methods, DP-CD-Net [110] introduces a dual-pathway change detection network that compromises a dual-pathway feature difference network, an adaptive fusion module, and an auxiliary supervision strategy. Different from SAR images, multispectral images, especially very-high-resolution images, tend to have a higher spatial resolution; thus, some region-based, object-based, and superpixel-based approaches have been proposed to achieve both homogeneous results and efficiency. To delve deeper into this topic, readers can refer to the survey paper [49] for additional details.

(3) Hyperspectral methods. Some of the representative literature on hyperspectral image change detection is shown in the third block of Table 3. Among the pixel-based methods, GETNET [81] presents a general end-to-end 2D CNN framework for hyperspectral image change detection. Wang et al. [111] propose an end-to-end Siamese CNN with a spectral–spatial-wise attention mechanism to emphasize informative channels and locations and suppress less informative ones to refine the spectral–spatial features adaptively. CDFormer [45] introduces a transformer encoder method for the hyperspectral image change detection tasks with space and time encodings, as well as a self-attention component. For the hybrid methods, FuzCVA [112] presents a new fuzzy inference combination strategy to combine the angle and magnitude distances, which can provide improved change detection performance. Luo et al. [83] propose a multiscale diff-changed feature fusion network, which combines a temporal feature encoder–decoder subnetwork and a cross-layer attention module.

(4) Heterogeneous methods. The fourth block of Table 3 displays a selection of the notable literature on techniques for detecting changes in heterogeneous data. Among the pixel-based methods, SCCN [27] presents a symmetric convolutional coupling network with a symmetrical structure and feature transformation. Li et al. [113] introduce a spatially self-paced convolutional network for change detection in an unsupervised way. For the region-based methods, MSGCN [114] proposes a new change detection method that combines a graph convolutional network and multiscale object-based technique for both homogeneous and heterogeneous images. Wan et al. [115] propose an improved change detection method that combines a cooperative multitemporal segmentation method and a region-based multitemporal hierarchical Markov random field model. For the hybrid methods, HMCNet [38] introduces a multilayer perceptron into CNNs for change detection tasks. Wang et al. [116] introduce a deep adversarial network to fuse a pair of multiband images, which can be easily complemented by a network with the same architecture to perform change detection.

(5) Three-dimensional change detection methods. The final block of Table 3 demonstrates some representative literature for 3D change detection tasks. Among the pixel-based methods, Marmol et al. [117] propose an algorithm that is based on height difference-generated

nDSM, including morphological filters and criteria considering area size and shape parameters. Chai et al. [118] present a 3D change detection method based on density adaptive local Euclidean distance, which includes calculating the local Euclidean distances from each point, improving the local geometric Euclidean distance based on the local density, and clustering the change detection results using Euclidean clustering. For the region-based methods, CHM-CD [119] introduces a method that first detects the large changes by comparing the canopy height models from the two LiDAR data, and then an object-based technique is utilized to obtain the change detection results.

In conclusion, pixel-based methods [20,105,121] include their ease of implementation, computational efficiency, and ability to identify small changes at high resolution, making them well-suited for detecting changes in homogeneous regions. However, these methods are not suitable for detecting changes in heterogeneous regions, do not capture spatial information, and are sensitive to noise. Region-based methods [105,106,122] are robust to noise and suitable for detecting changes in heterogeneous regions, as well as capturing spatial information such as the shape and size of changes, making them well suited for detecting changes in regions with complex spectral properties. The disadvantages of region-based methods for change detection include their computational intensity, sensitivity to the choice of segmentation algorithm, and potential ineffectiveness in detecting small changes, which may require expert knowledge to select appropriate segmentation parameters. Hybrid methods [106,112] combine the strengths of pixel-based and region-based methods, making them effective in detecting small and large changes in complex scenes as well as robust to noise and suitable for detecting changes in heterogeneous regions. Hybrid methods offer advantages such as effectiveness in detecting small and large changes in complex scenes, robustness to noise, and suitability for detecting changes in heterogeneous regions, while they have limitations such as computational intensity, sensitivity to the choice of segmentation algorithm, and potential ineffectiveness in detecting changes in regions with complex spectral properties, which may require a high degree of expertise to implement.

3.2. Taxonomy Based on Supervision Modes

Based on the supervision modes, the existing change detection algorithms can be categorized into three types: unsupervised learning, semisupervised learning, and supervised learning as follows:

- **Unsupervised learning.** Unsupervised learning is a machine learning technique that discovers patterns and structures in data without guidance or labels, enabling the identification of hidden relationships and structures without prior knowledge. However, it can be difficult to interpret. It may suffer from the "curse of dimensionality", where the number of features or dimensions of the data can lead to computational inefficiencies or inaccurate results.
- **Semisupervised learning.** Semisupervised learning aims at training the algorithm with a limited amount of labeled data and a large set of unlabeled data. It is advantageous when labeled data are scarce or expensive to obtain and can help improve model accuracy by leveraging unlabeled data. Still, its implementation can be difficult, and its performance depends on the quality of unlabeled data, which can introduce noise and lead to decreased performance.
- **Supervised learning.** Supervised learning is trained using labeled data to make accurate predictions on new, unseen data by learning patterns from input and corresponding output data. It is easy to implement with readily available labeled data and can be used to solve various problems, but it requires a large amount of labeled data that should be accurate and unbiased, and models may struggle with data different from the training data, leading to overfitting or underfitting.

In the following, we provide detailed and practical insights into change detection algorithms for each data source based on the modes of supervision, shown in Table 4.

Table 4. The representative literature on various supervision modes for different data sources in change detection tasks. We also illustrate the fusion category for each approach.

Method	Source	Category	Fusion	Highlights
SAR Methods				
SFCNet [123]	TGRS 2022	Unsupervised	Early	Proposes a sparse feature clustering network for unsupervised change detection in SAR images.
HFEM [75]	TGRS 2022	Unsupervised	Early	Introduces an unsupervised change detection method that contains three procedures: difference image generation, thresholding, and spatial analysis.
CycleGAN-CD [124]	TGRS 2021	Unsupervised	Middle	Introduces a SAR change detection method based on a cycle-consistent generative adversarial network.
Two-step [125]	GRSL 2022	Semisupervised	Middle	Presents a two-step semisupervised model based on representation learning and pseudo labels.
LCS-EnsemNet [126]	J-STARS 2021	Semisupervised	Early	Develops a semisupervised method with two separate branches by incorporating a label-consistent self-ensemble network.
SSN [127]	GRSL 2023	Supervised	Early	Proposes a Stockwell scattering network that combines a wavelet scattering network and Fourier scattering network.
STGCNet [128]	GRSL 2022	Supervised	Early	Introduces a deep spatial–temporal gray-level co-occurrence-aware convolutional neural network.
Multispectral Methods				
CAE [129]	TGRS 2022	Unsupervised	Late	Proposes an unsupervised change detection method that exploits multiresolution deep feature maps derived by a convolutional autoencoder.
PixSSLs [130]	TGRS 2022	Unsupervised	Late	Introduces a pixel-wise contrastive approach with pseudo-Siamese network.
GAN-CD [63]	TGRS 2021	Unsupervised	Late	Introduces a GAN-based procedure for unsupervised change detection in satellite images.
SSALN [131]	TGRS 2022	Semisupervised	Late	Proposes a semisupervised adaptive ladder network for change detection in remote sensing images.
RCL [132]	TGRS 2022	Semisupervised	Late	Proposes a reliable contrastive learning method for semisupervised remote sensing image change detection.
DifUnet++ [133]	GRSL 2022	Supervised	Early	Proposes an effective satellite image change detection network based on Unet++ and a differential pyramid.
SDMNet [134]	GRSL 2022	Supervised	Late	Proposes a deep-supervised dual discriminative metric network that is trained end-to-end for change detection in high-resolution images.
Hyperspectral Methods				
MD-HSI-CD [135]	J-STARS 2021	Unsupervised	Early	Proposes an unsupervised end-to-end framework that employs two model-driven methods for hyperspectral image change detection task.
BCG-Net [136]	TIP 2022	Unsupervised	Middle	Introduces an unsupervised hyperspectral multiclass change detection network based on binary change detection approaches.
S^2MCD [137]	IGARSS 2017	Semisupervised	Early	Proposes a new semisupervised framework that combines an unsupervised change representation technique and supervised classifiers.
RSCNet [138]	TGRS 2022	Supervised	Early	Proposes an end-to-end residual self-calibrated network to increase the accuracy of hyperspectral change detection task.
MP-ConvLSTM [139]	TGRS 2022	Supervised	Late	Proposes a multipath convolutional long short-term memory and multipath convolutional LSTM for hyperspectral image change detection task.
Heterogeneous Methods				
BASNet [140]	GRSL 2022	Unsupervised	Late	Introduces a new bipartite adversarial autoencoder with structural self-similarity for heterogeneous images.
ACE-Net [141]	TGRS 2022	Unsupervised	Late	Introduces two new network architectures trained with loss functions weighted by priors that reduce the impact of change pixels on the learning objective.
S^3N [142]	TGRS 2022	Semisupervised	Middle	Presents a new semisupervised Siamese network based on transfer learning.
M-UNet [66]	GRSL 2022	Supervised	Early	Introduces a heterogeneous image change detection task based on classical UNet.
DHFF [143]	J-STARS 2020	Supervised	Middle	Presents a new deep homogeneous feature fusion for heterogeneous image change detection based on image style transfer.
Three-Dimensional Change Detection Methods				
CamShift [144]	J-STARS 2016	Unsupervised	Late	Proposes a Pollock model with CamShift algorithm to segment connected components into individual trees.
CVA-CD [145]	GRSL 2022	Unsupervised	Late	Proposes an unsupervised change detection algorithm of lidar data based on polar change vector analysis.
Dual Stream [146]	Arxiv 2022	Supervised	Middle	Presents a UNet model for segmenting the buildings from the background.
Siamese KPConv [147]	ISPRS JPRS 2023	Supervised	Middle	Proposes a deep Siamese KPConv network that deals with raw 3D point cloud data to perform change detection and categorization.

(1) SAR methods. Due to the scarcity of publicly available SAR image change detection datasets, unsupervised learning methods have become prevalent. In particular, image clustering techniques and parameter-fixed feature extraction networks are commonly utilized. For instance, SFCNet [123] proposes a sparse feature clustering network for detecting changes in SAR images, which is pretrained with the multiobjective sparse feature learning model. HFEM [75] introduces a new change detection method for very few changes or even none-changed areas, which contains difference image generation, a thresholding method, and the one-conditional random fields method. CycleGAN-CD [124] presents a SAR change detection method based on a cycle-consistent generative adversarial network. For the semisupervised learning approaches, Wang et al. [125] propose a patch-based semisupervised method to detect changed pixels from limited training data, including unsupervised pretraining and iterative discrimination. LCS-EnsemNet [126] develops a semisupervised method based on a two-branch strategy by incorporating a label-consistent self-ensemble network. Within the category of supervised learning approaches, SSN [127] proposes a Stockwell scattering network that combines a wavelet scattering network and a Fourier scattering network. Zhang et al. [128] introduce a deep spatial–temporal gray-level co-occurrence-aware CNN, which can effectively mine the spatial–temporal information and obtain robust results.

(2) Multispectral methods. For the unsupervised learning-based approaches, Bergamasco et al. [129] introduce a new approach for unsupervised change detection, which leverages multiresolution deep feature maps obtained from a convolutional autoencoder. Chen et al. [130] propose a pseudo-Siamese network that is trained to obtain pixel-wise representations and to align features from shifted image pairs. Ren et al. [63] propose a new unsupervised change detection framework utilizing a generative adversarial network to generate many better co-registered images. For the semisupervised learning algorithms, SSALN [131] proposes a semisupervised adaptive ladder network for change detection in remote sensing images, which can update pseudo labels iteratively. Wang et al. [132] propose a reliable contrastive learning method for semisupervised remote sensing image change detection by selecting reliable samples according to the prediction uncertainty of unlabeled images and introducing the contrastive loss. Among the set of supervised learning models, Zhang et al. [133] propose an effective satellite image change detection network, DifUnet++, which takes a differential pyramid of two input images as the input and incorporates a side-out fusion strategy to predict the detection results. SDMNet [134] introduces a new end-to-end metric learning algorithm for remote sensing change detection tasks, which introduces a discriminative decoder network to aggregate multiscale and global contextual information to obtain discriminative consistent features and a discriminative implicit metric module to measure the distance between features to achieve the changes.

(3) Hyperspectral methods. Amongst unsupervised learning techniques, Li et al. [135] propose an unsupervised end-to-end framework that employs two model-driven methods for the hyperspectral image change detection task. BCG-Net [136] proposes an unsupervised hyperspectral multiclass change detection network based on the binary change detection approach, which aims to boost the multiclass change detection result and unmixing result. For the semisupervised learning algorithms, Liu et al. [137] introduce the semisupervised hyperspectral detection approach, which generates the pseudo-label samples from the state-of-the-art unsupervised change representation technique and classifies the changed regions and no-changed regions by a supervised classifier. Within the category of supervised learning algorithms, Wang et al. [138] introduce a residual self-calibrated network for the hyperspectral image change detection task, which adaptively builds interspatial and interspectral dependencies around each spatial location with fewer extra parameters and reduced complexity. Shi et al. [139] propose a multipath convolutional long short-term memory neural network for the hyperspectral change detection task, which introduces an efficient channel attention module to refine features of different paths.

(4) Heterogeneous methods. For the unsupervised learning methods, BASNet [140] proposes a new bipartite adversarial autoencoder with structural self-similarity for heteroge-

neous remote sensing images, which introduces a structural consistency loss to transform the images into a common domain and an adversarial loss to make image translation with a more consistent style. Luppino et al. [141] propose two novel network architectures that are trained using loss functions weighted by priors, which helps to minimize the effect of changing pixels on the overall learning objective. Within the category of semisupervised learning approaches, S^3N [142] proposes a new semisupervised Siamese network based on transfer learning, which takes the low- and high-level features separately and treats them differently. Amongst supervised learning techniques, Lv et al. [66] introduce a UNet model for the heterogeneous remote sensing image change detection task, which incorporates a multiscale convolution module into a U-Net backbone to cover the various sizes and shapes of ground targets. DHFF [143] proposes a deep homogeneous feature fusion method for heterogeneous image change detection tasks, which segregates the semantic content and the style features to perform the homogeneous transformation.

(5) Three-dimensional change detection methods. Within the unsupervised learning methods, Xiao et al. [144] propose a tree-shaped model for a continuously adaptive mean shift algorithm to classify the clustered components into individual trees, then the tree parameters are derived with a point-based method and a model-based method. Marinelli et al. [145] introduce a new unsupervised change detection algorithm in lidar point clouds, which utilizes a polar change vector analysis to automatically discriminate between the different classes of change. Among the supervised learning algorithms, Yadav et al. [146] propose a change detection model with U-Net for segmenting the buildings from the background, which utilizes an automatic method to reduce the 3D point clouds into a much smaller representation without losing necessary information. Siamese KPConv [147] presents a Siamese network to perform 3D point cloud change detection and categorization in a single step.

In summary, unsupervised learning methods excel in detecting changes without labeled data and accommodating diverse data sources, but their incapability of distinguishing true changes from noise restricts their performance in complex environments. Semisupervised learning methods leverage both labeled and unlabeled data to achieve better accuracy than unsupervised methods, but their effectiveness relies on the quality and quantity of labeled data. Supervised learning methods can achieve high accuracy in detecting changes with sufficient labeled data, but their inflexibility and dependence on labeled data can pose limitations in some scenarios, such as complex patterns and scarce labeled data.

3.3. Taxonomy Based on Learning Frameworks

This subsection presents a taxonomy of the existing change detection algorithms based on their learning frameworks, shown in Table 5. The taxonomy is divided into four categories: traditional methods, CNN-based methods, attention- or transformer-based methods, and Mamba methods. Traditional methods commonly utilize conventional clustering or classification algorithms, such as SVM [13,14,17], random forests [15], and MRF [3,22], to partition the data into changed and unchanged areas. Figure 5 presents some representative network structures in the deep learning field. CNN-based methods [148] use CNNs (shown in Figure 5a) to automatically learn feature representations from the data, enabling the capture of complex patterns and spatial dependencies between pixels. This approach has demonstrated improved performance over traditional methods. Attention- or transformer-based methods [149–153], also based on deep learning methods, employ self-attention mechanisms to weight different regions of the input images based on their relevance to the task or to capture long-range dependencies between pixels and generate feature representations (shown in Figure 5c). Some scholars [43] have attempted to combine CNN and transformer structures to leverage the advantages of both (shown in Figure 5b). These methods have demonstrated superior performance compared to both CNN-based methods and traditional methods, representing the new state of the art for change detection in remote sensing imagery. However, both architectures possess inherent limitations: CNNs often encounter constraints due to their limited receptive fields, which inhibits their ability to capture extensive spatial contexts, while transformers are computa-

tionally intensive. Recently, Mamba architectures [57,58] have demonstrated outstanding performance across various foundational tasks in the remote sensing area, such as image classification [154], hyperspectral image classification [155], image dense prediction [156], image change captioning [157], and change detection [59] (shown in Figure 5d). Chen et al. [59] first introduced the Mamba structure into the change detection task. By modifying the corresponding structure, it can address tasks such as binary change detection (BCD), semantic change detection (SCD), and building damage assessment (BDA). CDMamba [59], based on the Mamba structure, introduces local information, which can effectively combine global and local features for handling CD tasks.

Table 5. The representative literature on various learning frameworks for different data sources in change detection tasks. We also illustrate the fusion category for each approach.

Method	Source	Category	Fusion	Highlights
SAR Methods				
Yu et al. [158]	GRSL 2022	Traditional	Early	proposes a traditional approach that combines a symmetric similarity matrix, a Shannon entropy, and an image segmentation method based on MRF.
Liu et al. [159]	GRSL 2022	Traditional	Middle	proposes an unsupervised method to automatically select training samples and utilizes a well-trained RF classifier to achieve change detection result.
Vinholi et al. [160]	TGRS 2022	CNN	Early	presents two supervised change detection algorithms based on CNNs that use stacks of SAR images.
DDNet [161]	GRSL 2022	CNN	Middle	presents a dual-domain network to jointly exploit the spatial and frequency features for SAR change detection task.
MSDC [149]	TGRS 2022	A or T	Middle	proposes a unified framework that integrates unsupervised clustering with CNN to learn clustering-friendly feature representations
MACNet [150]	IGARSS 2022	A or T	Early	introduces a multiscale attention convolution network to exploit the spatial information of feature maps from different scales.
ASGF [151]	GRSL 2023	A or T	Early	proposes a new SAR image change detection algorithm that is based on an attention mechanism in the spatial domain and a gated linear unit in the frequency domain.
Multispectral Methods				
MDF CD [162]	GRSL 2022	Traditional	Early	presents a novel multiscale decision fusion method for unsupervised change detection approach based on Dempster–Shafer theory and modified conditional random field.
Fang et al. [163]	GRSL 2022	Traditional	Early	proposes an unsupervised change detection method for high spatial resolution images based on the weighted change vector analysis and the improved Markov random field.
ECFNet [164]	GRSL 2023	CNN	Middle	presents a simple and efficient network architecture, extraction, comparison, and fusion network for change detection in remote-sensing images.
Chen et al. [165]	TGRS 2022	CNN	Late	incorporates semantic supervision into the self-supervised learning framework for remote sensing image change detection.
UNet++ [148]	Remote Sensing 2019	CNN	Early	utilizes the improved UNet++ structure to learn the change map from scratch with encoder–decoder framework.
DMATNet [166]	TGRS 2022	A or T	Middle	presents a dual-feature mixed attention-based transformer network for remote sensing image change detection.
Chen et al. [43]	TGRS 2022	A or T	Middle	proposes a bitemporal image transformer to efficiently and effectively model contexts within the spatial-temporal domain.
PA-Former [167]	GRSL 2022	A or T	Middle	introduces an end-to-end PA-Former for building change detection that combines prior extraction and contextual fusion together.
ACAHNet [168]	TGRS 2023	A or T	Middle	proposes an asymmetric cross-attention hierarchical network by combining CNN and transformer in a series-parallel manner.
ChangeMamba [59]	Arxiv 2024	Mamba	Middle	proposes the first Mamba architecture for the change detection task, which introduces spatio-temporal relationship modeling mechanism to obtain accurate change information.
Hyperspectral Methods				
ACDA [169]	J-STARS 2021	Traditional	Late	Proposes a hyperspectral anomaly change detection algorithm based on autoencoder to enhance nonlinear representation.
SMSL [170]	TGRS 2022	Traditional	Middle	Introduces a sketched multiview subspace learning model for hyperspectral image anomalous change detection task.
MMSRC [171]	J-STARS 2022	CNN	Early	Proposes a new multidirection and multiscale spectral–spatial residual network for hyperspectral multiclass change detection.
SFBS-FFGNET [172]	TGRS 2022	CNN	Early	Proposes a CNN framework involving slow–fast band selection and feature fusion grouping for hyperspectral image change detection.
SST-Former [173]	TGRS 2022	A or T	Middle	Proposes a joint spectral, spatial, and temporal transformer for hyperspectral image change detection.
Dong et al. [174]	TGRS 2023	A or T	Middle	Proposes an abundance matrix correlation analysis network based on hierarchical multihead self-cross hybrid attention for hyperspectral change detection.
CSANet [175]	GRSL 2022	A or T	Middle	Proposes a new cross-temporal interaction symmetric attention network.
DPMs^{2}raN [176]	TGRS 2022	A or T	Middle	Proposes a deep multiscale pyramid network with spatial–spectral residual attention.

Table 5. *Cont.*

Method	Source	Category	Fusion	Highlights
Heterogeneous Methods				
SDA-HCD [177]	TGRS 2022	Traditional	Late	Introduces a spectral domain analysis for heterogeneous change detection.
Sun et al. [178]	TGRS 2022	Traditional	Middle	Proposes an unsupervised image regression method for change detection tasks based on the structure consistency.
CAE [179]	TNNLS 2022	CNN	Late	Proposes an unsupervised change detection method that contains a convolutional autoencoder and a commonality autoencoder.
TVRBN [180]	TGRS 2022	CNN	Middle	Proposes an unsupervised joint learning model based on a total variation regularization and bipartite CNNs.
DA-MSCDNet [181]	IJAEOG 2022	CNN	Middle	Introduces a domain adaptation and a multisource change detection network to process heterogeneous images.
TSCNet [182]	Remote Sensing 2023	A or T	Middle	Proposes a new topology-coupling algorithm for heterogeneous image change detection task.
Three-Dimensional Change Detection Methods				
Dai et al. [183]	Remote Sensing 2020	Traditional	Middle	Presents an unsupervised, object-based method for integrated building extraction and change detection with point cloud data.
Liu et al. [184]	ISPRS IJGI 2021	Traditional	Early	Introduces an approach for 3D change detection using point-based comparison.
ChangeGAN [185]	RAL 2021	CNN	Middle	Proposes a generative adversarial network architecture for point cloud change detection.

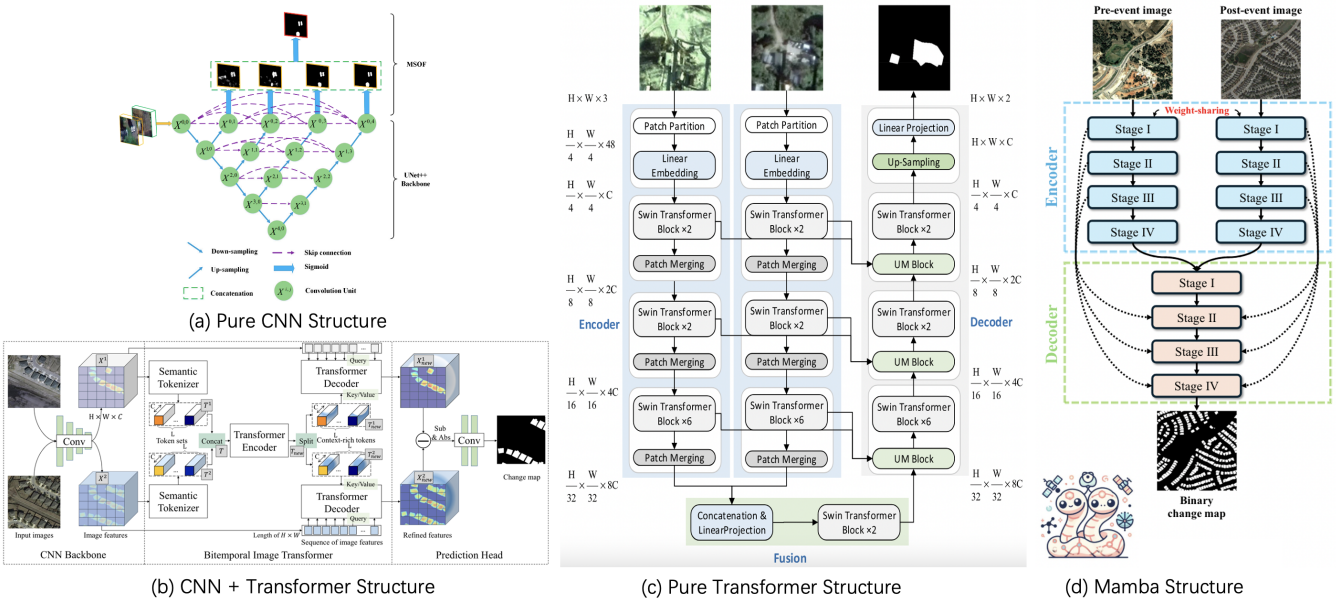

Figure 5. Some representative network structures in the change detection task. (**a**) Pure CNN structure [148], (**b**) CNN + transformer structure [43], (**c**) pure transformer structure [186], (**d**) Mamba structure [59].

(1) SAR methods. Among the traditional methods, Yu et al. [158] propose an unsupervised change detection algorithm, which combines a symmetric similarity matrix based on a likelihood ratio test, a Shannon entropy to calculate the difference image, and an image segmentation method based on MRF. Liu et al. [159] introduce an existing detection result to select the training data, a random forest classifier to achieve classification results, and median filtering to eliminate singular points. Within the CNN-based approaches, Vinholi et al. [160] present two supervised change detection algorithms based on CNNs, which consist of the following four stages: difference image formation, semantic segmentation, clustering, and change classification. DDNet [161] proposes a new SAR change detection method that uses features from both spatial and frequency domains. Specifically, a multiregion convolution module is utilized to enhance the spatial features, and a discrete cosine transform and

gating mechanism is employed to extract frequency features. In the category of attention- or transformer-based algorithms, MSDC [149] proposes an unsupervised change detection framework by combining K-means++ clustering and a deep convolutional model, which can be jointly optimized without supervision. Li et al. [150] present a multiscale attention convolution network, which extracts the spatial information of feature maps with a linear attention weight module, designs a linear attention weight module to emphasize the important channels adaptively, and fuses the contextual information from different scales. ASGF [151] proposes an unsupervised change detection approach, which employs a clustering technique to generate pseudo labels and utilizes a convolutional neural network to enable feature learning of the network.

(2) Multispectral methods. For traditional methods, Shao et al. [162] present a new multiscale decision fusion method for an unsupervised change detection approach based on Dempster–Shafer theory and a modified conditional random field, which consists of difference image generation, a fuzzy clustering algorithm, a fusion strategy based on Dempster–Shafer theory, and a modified CRF. Fang et al. [163] present an unsupervised approach for detecting changes in high-spatial-resolution images, which leverages the weighted change vector analysis technique and incorporates an improved Markov random field model. Among the set of CNN algorithms, ECFNet [164] proposes a simple but efficient network for remote sensing images, which consists of a feature extraction module, a feature comparison module, and a feature fusion module. Chen et al. [165] explore the use of semantic information in a representation learning framework and propose semantic-aware pretraining based on class-balanced sampling for remote sensing image change detection. UNet++ [148] introduces the improved UNet++ structure to learn the change information from scratch. Within the category of attention or transformer techniques, DMATNet [166] introduces a DFMA-based transformer change detection model for high-resolution remote sensing images, which utilizes CNNs to extract coarse and fine features and employs a dual-feature mixed attention (DFMA) module to fuse these features. Chen et al. [43] propose a bitemporal image transformer to efficiently and effectively model contexts within the spatial–temporal domain for remote sensing image change detection. PA-Former [167] presents a new network based on a transformer by learning a prior-aware transformer to help capture cross-temporal and long-range contextual information. ACAHNet [168] proposes an asymmetric cross-attention hierarchical network by combining a CNN and transformer in a series–parallel manner, which reduces the computational complexity and enhances the interaction between features extracted from the CNN and transformer.

(3) Hyperspectral methods. Among the traditional techniques, ACDA [169] introduces a new hyperspectral anomaly change detection algorithm based on a nonlinear autoencoder, which gains better detection performance against other state-of-the-art approaches. SMSL [170] introduces a sketched multiview subspace learning algorithm for anomalous change detection, which preserves major information from the image pairs and improves the computational complexity using a sketched representation matrix. Within the category of CNN methods, MMSRC [171] proposes a new multidirection and multiscale spectral–spatial residual network for hyperspectral multiclass change detection, which improves feature variation and accuracy of hyperspectral images. SFBS-FFGNET [172] introduces a CNN framework involving slow–fast band selection and feature fusion grouping for hyperspectral image change detection, which incorporates selecting effective bands and fusing different features. For the attention or transformer algorithms, SST-Former [173] introduces an end-to-end transformer model for the hyperspectral change detection task, which simultaneously considers the spatial, spectral, and temporal information for hyperspectral images. Dong et al. [174] propose an abundance matrix correlation analysis network based on hierarchical multihead self-cross hybrid attention for hyperspectral change detection, which hierarchically highlights the correlation difference information at the

subpixel level. CSANet [175] proposes a new cross-temporal interaction symmetric attention network, which can effectively extract and integrate the joint spatial–spectral–temporal features of the hyperspectral images and enhance the feature discrimination ability of the changes. DPMs^{2}raN [176] proposes a deep multiscale pyramid network with spatial–spectral residual attention, which has a strong capability to mine multilevel and multiscale spatial–spectral features, thus improving the performance in complex changed regions.

(4) Heterogeneous methods. For the traditional approaches, SDA-HCD [177] introduces a spectral domain analysis-based heterogeneous change detection, which decomposes the source signal into the regressed signal and the changed signal and constrains the spectral property of the regressed signal. Sun et al. [178] propose an unsupervised image regression-based change detection method based on the structure consistency, which uses a similarity graph to translate an image, computes the difference image, and then segments it into changed and unchanged classes using a superpixel-based Markovian segmentation model. Among the CNN methods, CAE [179] proposes an unsupervised change detection method that contains only a convolutional autoencoder for feature extraction and the commonality autoencoder for commonalities exploration. TVRBN [180] introduces an unsupervised joint learning model based on total variation regularization and bipartite CNN. DA-MSCDNet [181] proposes a domain adaptation-based multisource change detection network to process heterogeneous optical and SAR remote sensing images, which employs feature-level transformation to align inconsistent deep-feature spaces. Within the category of attention or transformer algorithms, TSCNet [182] introduces a new topology-coupling-based heterogeneous remote sensing image change detection network, which transforms the feature space of heterogeneous images using an encoder–decoder structure and introduces wavelet transform, channel, and spatial attention mechanisms.

(5) Three-dimensional change detection methods. For the traditional algorithms, Dai et al. [183] present an unsupervised, object-based method for integrated building extraction and change detection using point cloud data, which combines bottom-up segmentation and clustering as well as an object-based bidirectional algorithm. Liu et al. [184] propose an approach for 3D change detection using point-based comparison. To avoid density variation in point clouds, adaptive thresholds are calculated through the k-neighboring average distance and the local point cloud density. Among the CNN methods, ChangeGAN [185] introduces a generative adversarial network architecture for the point cloud change detection task, which combines Siamese-style feature extraction, U-net-like multiscale feature extraction, and spatial transformation network blocks for optimal transformation estimation. Siamese KPConv [147] proposes a deep Siamese KPConv network that deals with raw 3D PCs to perform change detection and categorization in a single step.

4. Benchmark Performance

In this section, we provide state-of-the-art methods for change detection tasks on the dominant datasets depicted in the preliminary knowledge section. It should be noted that we only present some representative algorithms that are commonly utilized for comparative analysis.

(1) SAR benchmarks. In Table 6, we provide a summary of several noteworthy methods on two dominant SAR datasets, i.e., the Yellow River dataset [74] and the Bern dataset [75]. Specifically, in the Yellow River dataset, the DDNet algorithm [161] outperforms other methods in terms of FP and KC metrics, while the SFCNet model [123] achieves the best performance on FN and OA metrics. In the Bern dataset, ShearNet [74] and ESMOFCM [187] exhibit superior performance, achieving an OA metric of 99.68%, and BIFLICM/D [188] achieves the best performance in the KC metric.

Table 6. Some representative methods on SAR datasets. The model with the best performance is denoted in bold.

SAR Methods					
Method	**Source**	**FP**	**FN**	**OA**	**KC**
Yellow River Dataset					
RFLICM [189]	TIP 2012	862	1300	98.33	74.97
GaborPCANet [190]	GRSL 2016	1043	1009	96.87	81.21
CWNNs [7]	GRSL 2019	837	1690	96.60	88.23
DCNet [191]	J-STARS 2019	790	2137	96.06	86.16
MSAPNet [192]	IGARSS 2020	817	2157	96.00	85.94
SFCNet [123]	TGRS 2022	720	**704**	**98.40**	85.62
SSN [127]	GRSL 2023	1292	793	97.19	90.66
DDNet [161]	GRSL 2022	**641**	1027	98.36	**93.77**
Bern Dataset					
GaborPCANet [190]	GRSL 2016	**36**	434	99.48	75.23
CWNNs [7]	GRSL 2019	81	226	99.66	85.56
ESMOFCM [187]	GRSL 2021	95	196	**99.68**	86.70
BIFLICM/D [188]	GRSL 2022	103	718	99.08	**91.24**
ShearNet [74]	TGRS 2022	163	**126**	**99.68**	87.41

(2) Multispectral benchmarks. Table 7 presents a collection of state-of-the-art models on several preeminent multispectral image datasets, including the LEVIR-CD+ dataset [76], the CDD dataset [193], the WHU-CD dataset [78], and the SECOND dataset [79]. Specifically, in the LEVIR-CD+ dataset, MambaBCD-Base [59] demonstrates superior performance across all evaluation metrics when compared to other methods. In the CDD dataset, P2V-CD [194] achieves the best performance of the F1 score, demonstrating superior results in both precision and recall metrics. Similarly, in the WHU-CD dataset, MambaBCD-Base [59] demonstrates remarkable performance, achieving the highest score in precision, F1, OA, and IoU. MambaBCD-Small [59] achieves the highest score in the recall metric. These findings indicate the effectiveness of MambaBCD in the analysis of multispectral remote sensing data for building extraction tasks. In the SECOND dataset with multiple change detection categories, SSESN [195] achieves the highest score for the OA metric, while MambaSCD-Base [59] achieves the highest performance for the metrics mIoU and Sek.

Table 7. Some representative methods on multispectral datasets. The model with the best performance is denoted in bold.

Multispectral Methods						
Method	**Source**	**Precision**	**Recall**	**F1**	**OA**	**IoU**
LEVIR-CD+ Dataset						
FC-EF [196]	ICIP 2018	69.12	71.77	70.42	97.54	54.34
SNUNet [197]	GRSL 2022	71.07	78.73	74.70	97.83	59.62
CGNet [198]	J-STARS 2023	81.46	86.02	83.68	98.63	71.94
ChangeFormerV3 [199]	IGARSS 2022	81.34	79.97	80.65	98.44	67.58
BIT-101 [43]	TGRS 2022	83.91	81.20	82.53	98.60	70.26
TransUNetCD [41]	TGRS 2022	83.08	84.18	83.63	98.66	71.86
SwinSUNet [186]	TGRS 2022	85.34	85.85	85.60	98.92	74.82
MambaBCD-Tiny [59]	Arxiv 2024	88.82	87.26	88.04	99.03	78.63
MambaBCD-Small [59]	Arxiv 2024	89.17	86.49	87.81	99.02	78.27
MambaBCD-Base [59]	Arxiv 2024	**89.24**	**87.57**	**88.39**	**99.06**	**79.20**

Table 7. *Cont.*

Multispectral Methods						
Method	**Source**	**Precision**	**Recall**	**F1**	**OA**	**IoU**
CDD Dataset						
FC-EF [196]	ICIP 2018	83.45	**98.47**	90.34	97.58	
STANet [76]	Remote Sensing 2020	95.17	92.88	94.01	–	
ESCNet [200]	TNNLS 2021	90.04	97.26	93.51	**98.45**	
ChangeFormer [199]	IGARSS 2022	94.50	93.51	94.23	–	
BIT [43]	TGRS 2022	96.07	93.49	94.76	–	
SNUNet [197]	GRSL 2022	98.09	97.42	97.75	–	
DSAMNet [80]	TGRS 2022	94.54	92.77	93.69	–	
P2V-CD [194]	TIP 2023	**98.57**	98.26	**98.42**	–	
WHU-CD Dataset						
FC-EF [196]	ICIP 2018	83.50	86.33	84.89	98.87	73.74
SNUNet [197]	GRSL 2022	88.04	87.36	87.70	99.10	78.09
CGNet [198]	J-STARS 2023	94.47	90.79	92.59	99.48	86.21
ChangeFormerV3 [199]	IGARSS 2022	88.25	85.55	86.88	99.05	76.80
BIT-101 [43]	TGRS 2022	89.83	90.24	90.04	99.27	81.88
TransUNetCD [41]	TGRS 2022	85.48	90.50	87.79	99.09	78.44
SwinSUNet [186]	TGRS 2022	94.08	92.03	93.04	99.50	87.00
MambaBCD-Tiny [59]	Arxiv 2024	94.76	91.94	93.33	99.52	87.49
MambaBCD-Small [59]	Arxiv 2024	95.90	**92.29**	94.06	99.57	88.79
MambaBCD-Base [59]	Arxiv 2024	**96.18**	92.23	**94.19**	**99.58**	**89.02**
SECOND Dataset						
Method	**Source**	**OA**	**mIoU**	**Sek**	F_{scd}	
HRSCD [201]	CVIU 2019	86.62	71.15	18.80	58.21	
ASN [79]	TGRS 2021	–	69.50	16.30	–	
SSCD [72]	TGRS 2022	87.19	72.60	21.86	61.22	
Bi-SRNet [72]	TGRS 2022	87.84	73.41	23.22	62.61	
SSESN [195]	J-STARS 2022	**89.00**	70.80	–	–	
MTSCD-Net [202]	IJAEOG 2023	87.04	71.68	20.57	–	
SCanNet [203]	TGRS 2024	87.76	73.42	23.94	63.66	
MambaSCD-Tiny [59]	Arxiv 2024	88.07	73.33	23.34	63.44	
MambaSCD-Small [59]	Arxiv 2024	88.38	73.61	24.04	**64.10**	
MambaSCD-Base [59]	Arxiv 2024	88.12	**73.68**	**24.11**	64.03	

(3) Hyperspectral benchmarks. In Table 8, we present some representative methods on two dominant hyperspectral datasets, i.e., the River dataset [81] and the Hermiston dataset [82]. Specifically, in the River dataset, MSDFFN [83] outperforms other methods with respect to the recall, F1 score, OA, and KC metrics. Meanwhile, SSA-SiamNet [111] achieves the highest precision score compared to all other evaluated methods. In the Hermiston dataset, MSDFFN [83] achieves the best performance in terms of precision, recall, F1 score, and OA metrics. Conversely, GETNET [81] achieves the best results in the KC metric compared to other methods.

Table 8. Some representative methods on hyperspectral datasets. The model with the best performance is denoted in bold.

Hyperspectral Methods						
Method	**Source**	**Precision**	**Recall**	**F1**	**OA**	**KC**
River Dataset						
PCAKM [204]	GRSL 2009	54.60	96.29	69.69	92.72	65.91
PCA-CVA [205]	GRSL 2016	–	–	–	95.16	74.77
GETNET [81]	TGRS 2018	85.64	78.98	82.18	97.18	80.53
SiamCRNN [206]	TGRS 2020	88.14	69.12	77.45	96.5	75.59
SSA-SiamNet [111]	TGRS 2021	**91.89**	74.10	82.04	97.18	80.53
ML-EDAN [36]	TGRS 2022	89.57	83.75	86.57	97.74	85.33
MSDFFN [83]	TGRS 2023	90.52	**87.58**	**89.01**	**98.12**	**87.98**
Hermiston Dataset						
PCAKM [204]	GRSL 2009	97.90	65.98	78.83	92.01	74.13
GETNET [81]	TGRS 2018	92.99	90.16	91.50	89.09	**96.23**
SiamCRNN [206]	TGRS 2020	92.66	49.28	62.67	87.35	56.15
SSA-SiamNet [111]	TGRS 2021	93.18	89.17	91.45	96.22	89.02
RSCNet [138]	TGRS 2022	93.98	91.32	92.63	96.73	90.53
ML-EDAN [36]	TGRS 2022	94.88	92.53	93.68	97.19	91.87
MSDFFN [83]	TGRS 2023	**95.55**	**93.69**	**94.61**	**97.59**	93.06
Farmland Dataset						
PCAKM [204]	GRSL 2009	89.78	93.96	91.82	95.14	88.37
GETNET [81]	TGRS 2018	95.64	97.40	96.51	97.96	**95.07**
SiamCRNN [206]	TGRS 2020	94.78	95.41	95.09	97.15	93.08
RSCNet [138]	TGRS 2022	97.33	96.96	97.15	98.35	95.98
ML-EDAN [138]	TGRS 2022	97.52	97.74	97.63	98.62	96.66
MSDFFN [83]	TGRS 2023	**97.79**	**97.77**	**97.78**	**98.71**	96.88

(4) Heterogeneous benchmarks. Table 9 presents several dominant methods that have been applied to the heterogeneous dataset, i.e., the California dataset [207]. Specifically, DPFL-Net-4 [207] demonstrates superior performance compared to other methods when evaluated based on the OA, KC, and AUC metrics. Notably, it achieves state-of-the-art results in all three metrics and particularly outperforms other methods by a significant margin in the KC metric.

Table 9. Some representative methods on heterogeneous datasets. The model with the best performance is denoted in bold.

Heterogeneous Methods					
Method	**Source**	**OA**	**KC**	**AUC**	**F1**
California Dataset					
SCCN [27]	TNNLS 2018	97.60	87.17	98.78	–
AM_HPT [208]	TGRS 2019	98.12	90.18	99.24	–
CAN [209]	GRSL 2019	90.40	36.50	–	42.40
ACE-Net [141]	TGRS 2021	91.50	41.50	–	**45.90**
CA_AE [84]	TNNLS 2022	97.88	88.66	99.18	–
DPFL-Net-4 [207]	TNNLS 2022	**98.89**	**94.17**	**99.79**	–

(5) Three-dimensional change detection benchmarks. Table 10 presents some representative models on the 3D change detection dataset, i.e., the 3DCD dataset [88]. To be specific, we find that MTBIT [88] achieves state-of-the-art performance in both the RMSE and cRMSE metrics.

Table 10. Some representative methods on 3D change detection datasets. The model with the best performance is denoted in bold.

Three-Dimensional Change Detection Methods			
Method	**Source**	**RMSE**	**cRMSE**
3DCD Dataset			
IM2HEIGHT [210]	ArXiv 2018	1.57	7.59
FC-EF [196]	ICIP 2018	1.41	7.04
ChangeFormer [199]	IGARSS 2022	1.31	7.09
SNUNet [197]	GRSL 2022	1.24	6.47
MTBIT [88]	ISPRS 2023	**1.20**	**6.46**

5. Future Trends

From the introduction of the methodology and benchmark evaluation, it is evident that networks for change detection based on the transformer and Mamba structures have achieved superior performance. However, there is still considerable room to further explore these structures. Particularly, how the Mamba structure can more effectively enhance the performance of change detection tasks is still in the early stages of research. It is believed that with further exploration, more optimal work will emerge. Currently, the following issues still exist in change detection tasks: (1) Due to limited data volumes and insufficient data diversity, the generality of mainstream change detection algorithms is inadequate, meaning that the trained models can only be used under specific spatial resolutions and sensors. (2) Current change detection models often produce false positives in areas with complex backgrounds or some slight background changes. (3) How to generate large datasets with a vast amount of high-quality annotated data, and utilizing these datasets to train universally applicable large change detection models, remains a worthwhile research problem that has not yet been well explored. In this section, we introduce several research trends that can be explored as follows:

Generalization of the change detection algorithms: The generalization performance of change detection algorithms in remote sensing is critical for their practical applications, as they need to be capable of effectively detecting changes in new and unobserved data, diverse geographical locations, different sensors, and varying environmental conditions. To improve their generalization, future trends include the use of transfer learning to transfer knowledge learned from one task or domain to others; domain adaptation [211] aims to adapt models to different environmental conditions or sensors; multisensor fusion to integrate data from different sensors; and explainable AI to interpret the decision-making process of a model. These trends are expected to enhance the generalization and overall performance of change detection algorithms in remote sensing images.

Learning with few samples: Few-shot learning [212,213] aims to train models with only a small amount of examples for each category, enabling them to generalize to new classes. The future trends in few-shot learning for change detection algorithms in remote sensing images include several key approaches, such as meta-learning, generative models, and domain generalization. Meta-learning involves enabling models to learn how to learn and quickly adapt to new classes. This approach allows models to leverage their past learning experiences and generalize to new tasks with fewer examples. Domain generalization [214] enables models to perform well on new and unseen domains. This approach involves training the model on data from different domains to improve its ability to generalize to new environments. By adapting to new geographical locations, sensors, or environmental conditions, these trends will enable algorithms to detect new types of changes with few ex-

amples, leading to better decision making and a deeper understanding of the environment. With the above strategies, similar performance can be achieved with only 1/3 or 1/4 of the annotation data, which can save a lot of annotation costs.

Deep dive in the transformer-based and Mamba-based algorithms: Transformer-based models [54,215–220] have achieved significant progress in computer vision. In particular, the self-attention-based methods [39,221,222] achieve better results than pure convolution-based methods for representation learning. The development of transformer-based algorithms for change detection in remote sensing images represents an emerging area of research with significant potential. To shape the future development of these algorithms, several trends have been identified, including the enhancement of attention mechanisms to better capture complex patterns and dependencies, integration with other deep learning models to create more robust and accurate change detection systems, and the use of unsupervised and semisupervised learning approaches to develop robust and accurate transformer models that can learn from unlabeled or partially labeled data. Additionally, future research will focus on the development of transformer models that can handle and integrate different data modalities, such as optical, radar, and LiDAR, to enhance the accuracy of change detection. Finally, online and continual learning approaches [223,224] will enable transformer models to learn and adapt to new data streams, allowing for more accurate and robust change detection systems. Additionally, Mamba architecture [59] has shown significant potential in change detection tasks. Therefore, further research on how to improve upon the Mamba architecture for model acceleration and performance accuracy enhancement, as well as considering the integration of Mamba with transformer structures, could also be some promising research directions.

Efficient models for practical applications: Efficiency is a crucial factor in developing practical and scalable change detection algorithms for remote sensing images. Here are some of the future trends in the development of efficient models for change detection: Sparse and lightweight models [225–229]: To reduce the computational complexity and memory footprint of change detection algorithms, future research will focus on developing sparse and lightweight models. These models will be designed to perform the change detection task with a minimal number of parameters and operations while maintaining high accuracy. Compression techniques [230,231]: Compression techniques such as pruning, quantization, and knowledge distillation can reduce the size of deep learning models without sacrificing performance. Future research will explore ways to apply these techniques to change detection models, reducing their memory and computational requirements.

Incorporate with synthetic data: To train a high-performing and generalized change detection model, a significant amount of labeled data is required, which in turn demands substantial manual efforts for data collection and annotation. One possible solution is to employ a generated synthetic dataset. Recently, diffusion-based generation models [55,232] have provided the opportunity to create higher-quality images and corresponding masks than previous generative models. For instance, DDPM-CD [233] leverages off-the-shelf, unlabeled remote sensing images in the training process by pretraining a denoising diffusion probabilistic model (DDPM) for the change detection task. TransC-GD-CD [234] utilizes a transformer-based conditional generative diffusion method for the CD task, tailored for generating CD data, which leverages the numerous sampling iterations of the DDPM, contributing to the generation of high-quality CD maps. Generative images with diffusion models exhibit fewer domain gaps than real images, offering greater potential for training change detection models without reliance on real data. Furthermore, depending on the specific application scenarios, generative images, and masks can be produced to cater to task-specific needs, including few-shot or long-tail tasks.

Integration of multisource/modal and multiple datasets: As delineated in the preliminary section, numerous datasets exist for each data source. A plausible approach to enhancing model performance and generality is amalgamating these datasets for each data source to create a more extensive change detection dataset. It is important to recognize that dissimilarities may exist among datasets from different domains. Thus, minimizing these

domain gaps represents another research concern. Additionally, further research could be conducted to investigate cross-domain multisource datasets [235] in order to improve model training. For instance, one could explore methods for distilling the knowledge [236] acquired from a vast amount of multispectral change data into secrecy SAR data, thereby achieving superior performance on corresponding SAR data. One potential avenue for future research is to explore the integration of multimodal data, specifically the incorporation of image and text pairs, to improve the accuracy of selected area change detection. It is possible that the creation of a large-scale image–text-based change detection dataset could facilitate progress in this direction. This approach could provide a more comprehensive understanding of changes occurring in a given area by incorporating both visual and textual data. The utilization of multimodal data has been shown to be effective in other areas of research, and it is possible that this approach could yield promising results in the field of selected area change detection. Further investigation in this direction may help to identify new patterns and insights related to selected area change detection.

Exploration based on foundation models: Recently, there has been a surge in the development of foundation models, such as Segment Anything [237], Painter [238], and SegGPT [239], that leverage large amounts of data and GPU resources. For example, Segment Anything, also known as SAM, is a highly effective method for segmenting all types of targets, making it highly versatile for remote sensing applications, especially for high-resolution images. To further improve change detection tasks, there are two promising research avenues. First, an automatic approach can be developed to generate a more extensive change detection dataset, which can help train more comprehensive aerial-specific foundation models. Second, integrating foundation models can address domain adaptation gaps and significantly enhance change detection performance.

6. Conclusions

This paper provides a comprehensive and in-depth survey of the recent advancements in change detection for remote sensing images which have been achieved over the past decade. Through the comprehensive review of fundamental knowledge and the classification of existing algorithms, this paper provides a detailed and organized understanding of the current state of the field. Additionally, the summary of the state-of-the-art performance on several datasets demonstrates the effectiveness of deep learning techniques in addressing the challenges of change detection. Finally, the identification of future research directions provides valuable insights into the potential avenues for further advancement of the field. It is our sincere hope that this survey paper will not only contribute to the current understanding of change detection in remote sensing but also inspire and guide future research efforts in this area.

Author Contributions: Conceptualization, G.C. and X.L.; methodology, G.C., Y.H. and X.L.; software, G.C. and Y.H.; validation, G.C., Y.H. and S.L.; formal analysis, G.C. and Y.H.; data curation, G.C. and Y.H.; writing—original draft preparation, G.C., Y.H., X.L. and Z.X.; writing—review and editing, Q.Z., S.X. and H.Z.; visualization, G.C., Z.X. and Y.H.; supervision, S.X., Q.Z. and H.Z.; All authors have read and agreed to the published version of the manuscript.

Funding: This research received no external funding.

Data Availability Statement: No new data were created in this manuscript.

Conflicts of Interest: The authors declare no conflicts of interest.

References

1. Buch, N.E.; Velastin, S.A.; Orwell, J. A Review of Computer Vision Techniques for the Analysis of Urban Traffic. *IEEE Trans. Intell. Transp. Syst.* **2011**, *12*, 920–939. [CrossRef]
2. Liu, Y.; Pang, C.; Zhan, Z.; Zhang, X.; Yang, X. Building Change Detection for Remote Sensing Images Using a Dual-Task Constrained Deep Siamese Convolutional Network Model. *IEEE Geosci. Remote Sens. Lett.* **2021**, *18*, 811–815. [CrossRef]
3. Bruzzone, L.; Fernández-Prieto, D. Automatic analysis of the difference image for unsupervised change detection. *IEEE Trans. Geosci. Remote Sens.* **2000**, *38*, 1171–1182. [CrossRef]

4. Liu, M.; Chai, Z.; Deng, H.; Liu, R. A CNN-Transformer Network With Multiscale Context Aggregation for Fine-Grained Cropland Change Detection. *IEEE J. Sel. Top. Appl. Earth Obs. Remote Sens.* **2022**, *15*, 4297–4306. [CrossRef]
5. Shi, S.; Zhong, Y.; Zhao, J.; Lv, P.; Liu, Y.; Zhang, L. Land-Use/Land-Cover Change Detection Based on Class-Prior Object-Oriented Conditional Random Field Framework for High Spatial Resolution Remote Sensing Imagery. *IEEE Trans. Geosci. Remote Sens.* **2022**, *60*, 5600116. [CrossRef]
6. Khan, S.H.; He, X.; Porikli, F.; Bennamoun, M. Forest Change Detection in Incomplete Satellite Images with Deep Neural Networks. *IEEE Trans. Geosci. Remote Sens.* **2017**, *55*, 5407–5423. [CrossRef]
7. Gao, F.; Wang, X.; Gao, Y.; Dong, J.; Wang, S. Sea Ice Change Detection in SAR Images Based on Convolutional-Wavelet Neural Networks. *IEEE Geosci. Remote Sens. Lett.* **2019**, *16*, 1240–1244. [CrossRef]
8. Brunner, D.; Bruzzone, L.; Lemoine, G. Change detection for earthquake damage assessment in built-up areas using very high resolution optical and SAR imagery. In Proceedings of the IEEE International Geoscience & Remote Sensing Symposium, IGARSS, Honolulu, HI, USA, 25–30 July 2010; IEEE: Piscataway, NJ, USA, 2010; pp. 3210–3213.
9. Gong, M.; Zhao, J.; Liu, J.; Miao, Q.; Jiao, L. Change Detection in Synthetic Aperture Radar Images Based on Deep Neural Networks. *IEEE Trans. Neural Netw. Learn. Syst.* **2016**, *27*, 125–138. [CrossRef]
10. Shafique, A.; Cao, G.; Khan, Z.; Asad, M.; Aslam, M. Deep Learning-Based Change Detection in Remote Sensing Images: A Review. *Remote Sens.* **2022**, *14*, 871. [CrossRef]
11. Jiang, H.; Peng, M.; Zhong, Y.; Xie, H.; Hao, Z.; Lin, J.; Ma, X.; Hu, X. A Survey on Deep Learning-Based Change Detection from High Resolution Remote Sensing Images. *Remote Sens.* **2022**, *14*, 1552. [CrossRef]
12. Zhu, Q.; Guo, X.; Li, Z.; Li, D. A review of multi-class change detection for satellite remote sensing imagery. *Geo-Spat. Inf. Sci.* **2022**, *27*, 1–15. [CrossRef]
13. Huo, C.; Chen, K.; Ding, K.; Zhou, Z.; Pan, C. Learning Relationship for Very High Resolution Image Change Detection. *IEEE J. Sel. Top. Appl. Earth Obs. Remote Sens.* **2016**, *9*, 3384–3394. [CrossRef]
14. Bovolo, F.; Bruzzone, L.; Marconcini, M. A Novel Approach to Unsupervised Change Detection Based on a Semisupervised SVM and a Similarity Measure. *IEEE Trans. Geosci. Remote Sens.* **2008**, *46*, 2070–2082. [CrossRef]
15. Seo, D.K.; Kim, Y.; Eo, Y.D.; Lee, M.H.; Park, W.Y. Fusion of SAR and Multispectral Images Using Random Forest Regression for Change Detection. *ISPRS Int. J. Geo Inf.* **2018**, *7*, 401. [CrossRef]
16. Xie, Z.; Wang, M.; Han, Y.; Yang, D. Hierarchical Decision Tree for Change Detection Using High Resolution Remote Sensing Images. In Proceedings of the Geo-Informatics in Sustainable Ecosystem and Society, Handan, China, 25–26 September 2018; Xie, Y., Zhang, A., Liu, H., Feng, L., Eds.; Communications in Computer and Information Science; Springer: Berlin/Heidelberg, Germany, 2016; Volume 980, pp. 176–184.
17. Cao, G.; Li, Y.; Liu, Y.; Shang, Y. Automatic change detection in high-resolution remote-sensing images by means of level set evolution and support vector machine classification. *Int. J. Remote Sens.* **2014**, *35*, 6255–6270. [CrossRef]
18. Hao, M.; Shi, W.; Zhang, H.; Li, C. Unsupervised Change Detection with Expectation-Maximization-Based Level Set. *IEEE Geosci. Remote Sens. Lett.* **2014**, *11*, 210–214. [CrossRef]
19. Li, H.; Li, M.; Zhang, P.; Song, W.; An, L.; Wu, Y. SAR Image Change Detection Based on Hybrid Conditional Random Field. *IEEE Geosci. Remote Sens. Lett.* **2015**, *12*, 910–914.
20. Hao, M.; Zhou, M.; Jin, J.; Shi, W. An Advanced Superpixel-Based Markov Random Field Model for Unsupervised Change Detection. *IEEE Geosci. Remote Sens. Lett.* **2020**, *17*, 1401–1405. [CrossRef]
21. Zhou, L.; Cao, G.; Li, Y.; Shang, Y. Change Detection Based on Conditional Random Field with Region Connection Constraints in High-Resolution Remote Sensing Images. *IEEE J. Sel. Top. Appl. Earth Obs. Remote Sens.* **2016**, *9*, 3478–3488. [CrossRef]
22. Touati, R.; Mignotte, M.; Dahmane, M. Multimodal Change Detection in Remote Sensing Images Using an Unsupervised Pixel Pairwise-Based Markov Random Field Model. *IEEE Trans. Image Process.* **2020**, *29*, 757–767. [CrossRef]
23. Zhu, X.X.; Tuia, D.; Mou, L.; Xia, G.S.; Zhang, L.; Xu, F.; Fraundorfer, F. Deep Learning in Remote Sensing: A Comprehensive Review and List of Resources. *IEEE Geosci. Remote Sens. Mag.* **2017**, *5*, 8–36. [CrossRef]
24. Zhang, L.; Zhang, L.; Du, B. Deep Learning for Remote Sensing Data: A Technical Tutorial on the State of the Art. *IEEE Geosci. Remote Sens. Mag.* **2016**, *4*, 22–40. [CrossRef]
25. Zhan, Y.; Fu, K.; Yan, M.; Sun, X.; Wang, H.; Qiu, X. Change Detection Based on Deep Siamese Convolutional Network for Optical Aerial Images. *IEEE Geosci. Remote Sens. Lett.* **2017**, *14*, 1845–1849. [CrossRef]
26. Huang, R.; Zhou, M.; Xing, Y.; Zou, Y.; Fan, W. Change detection with various combinations of fluid pyramid integration networks. *Neurocomputing* **2021**, *437*, 84–94. [CrossRef]
27. Liu, J.; Gong, M.; Qin, A.K.; Zhang, P. A Deep Convolutional Coupling Network for Change Detection Based on Heterogeneous Optical and Radar Images. *IEEE Trans. Neural Netw. Learn. Syst.* **2018**, *29*, 545–559. [CrossRef] [PubMed]
28. Hou, B.; Liu, Q.; Wang, H.; Wang, Y. From W-Net to CDGAN: Bitemporal Change Detection via Deep Learning Techniques. *IEEE Trans. Geosci. Remote Sens.* **2020**, *58*, 1790–1802. [CrossRef]
29. Khurana, M.; Saxena, V. A Unified Approach to Change Detection Using an Adaptive Ensemble of Extreme Learning Machines. *IEEE Geosci. Remote Sens. Lett.* **2020**, *17*, 794–798. [CrossRef]
30. Kerner, H.R.; Wagstaff, K.L.; Bue, B.D.; Gray, P.C.; III, J.F.B.; Amor, H.B. Toward Generalized Change Detection on Planetary Surfaces With Convolutional Autoencoders and Transfer Learning. *IEEE J. Sel. Top. Appl. Earth Obs. Remote Sens.* **2019**, *12*, 3900–3918. [CrossRef]

31. Zhao, W.; Mou, L.; Chen, J.; Bo, Y.; Emery, W.J. Incorporating Metric Learning and Adversarial Network for Seasonal Invariant Change Detection. *IEEE Trans. Geosci. Remote Sens.* **2020**, *58*, 2720–2731. [CrossRef]
32. Lin, Y.; Li, S.; Fang, L.; Ghamisi, P. Multispectral Change Detection with Bilinear Convolutional Neural Networks. *IEEE Geosci. Remote Sens. Lett.* **2020**, *17*, 1757–1761. [CrossRef]
33. Vaswani, A.; Shazeer, N.; Parmar, N.; Uszkoreit, J.; Jones, L.; Gomez, A.N.; Kaiser, L.; Polosukhin, I. Attention is All you Need. In Proceedings of the Advances in Neural Information Processing Systems 2017, Long Beach, CA, USA, 4–9 December 2017; pp. 5998–6008.
34. Wang, Z.; Jiang, F.; Liu, T.; Xie, F.; Li, P. Attention-Based Spatial and Spectral Network with PCA-Guided Self-Supervised Feature Extraction for Change Detection in Hyperspectral Images. *Remote Sens.* **2021**, *13*, 4927. [CrossRef]
35. Gong, M.; Jiang, F.; Qin, A.K.; Liu, T.; Zhan, T.; Lu, D.; Zheng, H.; Zhang, M. A Spectral and Spatial Attention Network for Change Detection in Hyperspectral Images. *IEEE Trans. Geosci. Remote Sens.* **2022**, *60*, 5521614. [CrossRef]
36. Qu, J.; Hou, S.; Dong, W.; Li, Y.; Xie, W. A Multilevel Encoder-Decoder Attention Network for Change Detection in Hyperspectral Images. *IEEE Trans. Geosci. Remote Sens.* **2022**, *60*, 5518113. [CrossRef]
37. Meng, D.; Gao, F.; Dong, J.; Du, Q.; Li, H. Synthetic Aperture Radar Image Change Detection via Layer Attention-Based Noise-Tolerant Network. *IEEE Geosci. Remote Sens. Lett.* **2022**, *19*, 4026505. [CrossRef]
38. Wang, L.; Li, H. HMCNet: Hybrid Efficient Remote Sensing Images Change Detection Network Based on Cross-Axis Attention MLP and CNN. *IEEE Trans. Geosci. Remote Sens.* **2022**, *60*, 1–14. [CrossRef]
39. Dosovitskiy, A.; Beyer, L.; Kolesnikov, A.; Weissenborn, D.; Zhai, X.; Unterthiner, T.; Dehghani, M.; Minderer, M.; Heigold, G.; Gelly, S.; et al. An Image is Worth 16 × 16 Words: Transformers for Image Recognition at Scale. In Proceedings of the International Conference on Learning Representations, ICLR 2021, Virtual Event, Austria, 3–7 May 2021.
40. Huang, R.; Wang, R.; Guo, Q.; Zhang, Y.; Fan, W. IDET: Iterative Difference-Enhanced Transformers for High-Quality Change Detection. *arXiv* **2022**, arXiv:2207.09240.
41. Li, Q.; Zhong, R.; Du, X.; Du, Y. TransUNetCD: A Hybrid Transformer Network for Change Detection in Optical Remote-Sensing Images. *IEEE Trans. Geosci. Remote Sens.* **2022**, *60*, 5622519. [CrossRef]
42. Song, X.; Hua, Z.; Li, J. PSTNet: Progressive Sampling Transformer Network for Remote Sensing Image Change Detection. *IEEE J. Sel. Top. Appl. Earth Obs. Remote Sens.* **2022**, *15*, 8442–8455. [CrossRef]
43. Chen, H.; Qi, Z.; Shi, Z. Remote Sensing Image Change Detection with Transformers. *IEEE Trans. Geosci. Remote Sens.* **2022**, *60*, 1–14. [CrossRef]
44. Song, F.; Zhang, S.; Lei, T.; Song, Y.; Peng, Z. MSTDSNet-CD: Multiscale Swin Transformer and Deeply Supervised Network for Change Detection of the Fast-Growing Urban Regions. *IEEE Geosci. Remote Sens. Lett.* **2022**, *19*, 1–5. [CrossRef]
45. Ding, J.; Li, X.; Zhao, L. CDFormer: A Hyperspectral Image Change Detection Method Based on Transformer Encoders. *IEEE Geosci. Remote Sens. Lett.* **2022**, *19*, 1–5. [CrossRef]
46. Lu, K.; Huang, X. RCDT: Relational Remote Sensing Change Detection with Transformer. *arXiv* **2022**, arXiv:2212.04869.
47. Khan, S.H.; Naseer, M.; Hayat, M.; Zamir, S.W.; Khan, F.S.; Shah, M. Transformers in Vision: A Survey. *ACM Comput. Surv.* **2022**, *54*, 200:1–200:41. [CrossRef]
48. Gangi, M.A.D.; Negri, M.; Turchi, M. Adapting Transformer to End-to-End Spoken Language Translation. In Proceedings of the Interspeech 2019, 20th Annual Conference of the International Speech Communication Association, Graz, Austria, 15–19 September 2019; Kubin, G., Kacic, Z., Eds.; ISCA: Haymarket, Australia, 2019; pp. 1133–1137.
49. You, Y.; Cao, J.; Zhou, W. A Survey of Change Detection Methods Based on Remote Sensing Images for Multi-Source and Multi-Objective Scenarios. *Remote Sens.* **2020**, *12*, 2460. [CrossRef]
50. Afaq, Y.; Manocha, A. Analysis on change detection techniques for remote sensing applications: A review. *Ecol. Inform.* **2021**, *63*, 101310. [CrossRef]
51. Stilla, U.; Xu, Y. Change detection of urban objects using 3D point clouds: A review. *ISPRS J. Photogramm. Remote Sens.* **2023**, *197*, 228–255. [CrossRef]
52. Li, J.; Zhu, S.; Gao, Y.; Zhang, G.; Xu, Y. Change Detection for High-Resolution Remote Sensing Images Based on a Multi-Scale Attention Siamese Network. *Remote Sens.* **2022**, *14*, 3464. [CrossRef]
53. Zhou, Q.; Li, X.; He, L.; Yang, Y.; Cheng, G.; Tong, Y.; Ma, L.; Tao, D. TransVOD: End-to-end Video Object Detection with Spatial-Temporal Transformers. *arXiv* **2022**, arXiv:2201.05047.
54. Li, X.; Ding, H.; Zhang, W.; Yuan, H.; Pang, J.; Cheng, G.; Chen, K.; Liu, Z.; Loy, C.C. Transformer-Based Visual Segmentation: A Survey. *arXiv* **2023**, arXiv:2304.09854.
55. Dhariwal, P.; Nichol, A.Q. Diffusion Models Beat GANs on Image Synthesis. In Proceedings of the NeurIPS 2021, online, 6–14 December 2021; pp. 8780–8794.
56. Yang, L.; Zhang, Z.; Song, Y.; Hong, S.; Xu, R.; Zhao, Y.; Shao, Y.; Zhang, W.; Yang, M.; Cui, B. Diffusion Models: A Comprehensive Survey of Methods and Applications. *arXiv* **2022**, arXiv:2209.00796.
57. Liu, Y.; Tian, Y.; Zhao, Y.; Yu, H.; Xie, L.; Wang, Y.; Ye, Q.; Liu, Y. VMamba: Visual State Space Model. *arXiv* **2024**, arXiv:2401.10166.
58. Zhu, L.; Liao, B.; Zhang, Q.; Wang, X.; Liu, W.; Wang, X. Vision Mamba: Efficient Visual Representation Learning with Bidirectional State Space Model. *arXiv* **2024**, arXiv:2401.09417.
59. Chen, H.; Song, J.; Han, C.; Xia, J.; Yokoya, N. ChangeMamba: Remote Sensing Change Detection with Spatio-Temporal State Space Model. *arXiv* **2024**, arXiv:2404.03425.

60. Lillestrand, R.L. Techniques for Change Detection. *IEEE Trans. Comput.* **1972**, *21*, 654–659. [CrossRef]
61. Lu, D.; Mausel, P.; Brondízio, E.; Moran, E. Change detection techniques. *Int. J. Remote Sens.* **2004**, *25*, 2365–2401. [CrossRef]
62. Shi, W.; Zhang, M.; Zhang, R.; Chen, S.; Zhan, Z. Change Detection Based on Artificial Intelligence: State-of-the-Art and Challenges. *Remote Sens.* **2020**, *12*, 1688. [CrossRef]
63. Ren, C.; Wang, X.; Gao, J.; Zhou, X.; Chen, H. Unsupervised Change Detection in Satellite Images with Generative Adversarial Network. *IEEE Trans. Geosci. Remote Sens.* **2021**, *59*, 10047–10061. [CrossRef]
64. Li, Z.; Tang, C.; Liu, X.; Zhang, W.; Dou, J.; Wang, L.; Zomaya, A.Y. Lightweight Remote Sensing Change Detection with Progressive Feature Aggregation and Supervised Attention. *IEEE Trans. Geosci. Remote Sens.* **2023**, *61*, 5602812. [CrossRef]
65. Yuan, J.; Wang, L.; Cheng, S. STransUNet: A Siamese TransUNet-Based Remote Sensing Image Change Detection Network. *IEEE J. Sel. Top. Appl. Earth Obs. Remote Sens.* **2022**, *15*, 9241–9253. [CrossRef]
66. Lv, Z.; Huang, H.; Gao, L.; Benediktsson, J.A.; Zhao, M.; Shi, C. Simple Multiscale UNet for Change Detection with Heterogeneous Remote Sensing Images. *IEEE Geosci. Remote Sens. Lett.* **2022**, *19*, 2504905. [CrossRef]
67. Rahmon, G.; Bunyak, F.; Seetharaman, G.; Palaniappan, K. Evaluation of Different Decision Fusion Mechanisms for Robust Moving Object Detection. In Proceedings of the 49th IEEE Applied Imagery Pattern Recognition Workshop, AIPR 2020, Washington DC, DC, USA, 13–15 October 2020; IEEE: Piscataway, NJ, USA, 2020; pp. 1–7.
68. Radke, R.J.; Andra, S.; Al-Kofahi, O.; Roysam, B. Image change detection algorithms: A systematic survey. *IEEE Trans. Image Process.* **2005**, *14*, 294–307. [CrossRef] [PubMed]
69. Alvarez, J.L.H.; Ravanbakhsh, M.; Demir, B. S2-CGAN: Self-Supervised Adversarial Representation Learning for Binary Change Detection in Multispectral Images. In Proceedings of the IGARSS, Waikoloa, HI, USA, 26 September 2020–2 October 2020; IEEE: Piscataway, NJ, USA, 2020; pp. 2515–2518.
70. Lv, Z.; Liu, T.; Benediktsson, J.A. Object-Oriented Key Point Vector Distance for Binary Land Cover Change Detection Using VHR Remote Sensing Images. *IEEE Trans. Geosci. Remote Sens.* **2020**, *58*, 6524–6533. [CrossRef]
71. Shiqi, T.; Ailong, M.; Zhuo, Z.; Yanfei, Z. Hi-UCD: A large-scale dataset for urban semantic change detection in remote sensing imagery. *arXiv* **2020**, arXiv:2011.03247.
72. Ding, L.; Guo, H.; Liu, S.; Mou, L.; Zhang, J.; Bruzzone, L. Bi-Temporal Semantic Reasoning for the Semantic Change Detection in HR Remote Sensing Images. *IEEE Trans. Geosci. Remote Sens.* **2022**, *60*, 5620014. [CrossRef]
73. Peng, D.; Bruzzone, L.; Zhang, Y.; Guan, H.; He, P. SCDNET: A novel convolutional network for semantic change detection in high resolution optical remote sensing imagery. *Int. J. Appl. Earth Obs. Geoinf.* **2021**, *103*, 102465. [CrossRef]
74. Dong, H.; Jiao, L.; Ma, W.; Liu, F.; Liu, X.; Li, L.; Yang, S. Deep Shearlet Network for Change Detection in SAR Images. *IEEE Trans. Geosci. Remote Sens.* **2022**, *60*, 5241115. [CrossRef]
75. Zhang, K.; Lv, X.; Chai, H.; Yao, J. Unsupervised SAR Image Change Detection for Few Changed Area Based on Histogram Fitting Error Minimization. *IEEE Trans. Geosci. Remote Sens.* **2022**, *60*, 5231819. [CrossRef]
76. Chen, H.; Shi, Z. A Spatial-Temporal Attention-Based Method and a New Dataset for Remote Sensing Image Change Detection. *Remote Sens.* **2020**, *12*, 1662. [CrossRef]
77. Lebedev, M.; Vizilter, Y.V.; Vygolov, O.; Knyaz, V.A.; Rubis, A.Y. Change detection in remote sensing images using conditional adversarial networks. *Int. Arch. Photogramm. Remote Sens. Spat. Inf. Sci.* **2018**, *XLII-2*, 565–571.
78. Ji, S.; Wei, S.; Lu, M. Fully Convolutional Networks for Multisource Building Extraction From an Open Aerial and Satellite Imagery Data Set. *IEEE Trans. Geosci. Remote Sens.* **2019**, *57*, 574–586. [CrossRef]
79. Yang, K.; Xia, G.; Liu, Z.; Du, B.; Yang, W.; Pelillo, M.; Zhang, L. Asymmetric Siamese Networks for Semantic Change Detection in Aerial Images. *IEEE Trans. Geosci. Remote Sens.* **2022**, *60*, 5609818. [CrossRef]
80. Shi, Q.; Liu, M.; Li, S.; Liu, X.; Wang, F.; Zhang, L. A Deeply Supervised Attention Metric-Based Network and an Open Aerial Image Dataset for Remote Sensing Change Detection. *IEEE Trans. Geosci. Remote Sens.* **2022**, *60*, 5604816. [CrossRef]
81. Wang, Q.; Yuan, Z.; Du, Q.; Li, X. GETNET: A General End-to-End 2-D CNN Framework for Hyperspectral Image Change Detection. *IEEE Trans. Geosci. Remote Sens.* **2019**, *57*, 3–13. [CrossRef]
82. Wang, L.; Wang, L.; Wang, H.; Wang, X.; Bruzzone, L. SPCNet: A Subpixel Convolution-Based Change Detection Network for Hyperspectral Images with Different Spatial Resolutions. *IEEE Trans. Geosci. Remote Sens.* **2022**, *60*, 5533314. [CrossRef]
83. Luo, F.; Zhou, T.; Liu, J.; Guo, T.; Gong, X.; Ren, J. Multiscale Diff-Changed Feature Fusion Network for Hyperspectral Image Change Detection. *IEEE Trans. Geosci. Remote Sens.* **2023**, *61*, 5502713. [CrossRef]
84. Luppino, L.T.; Hansen, M.A.; Kampffmeyer, M.; Bianchi, F.M.; Moser, G.; Jenssen, R.; Anfinsen, S.N. Code-Aligned Autoencoders for Unsupervised Change Detection in Multimodal Remote Sensing Images. *IEEE Trans. Neural Netw. Learn. Syst.* **2022**, *35*, 60–72. [CrossRef]
85. Coletta, V.; Marsocci, V.; Ravanelli, R. 3DCD: A new dataset for 2d and 3d change detection using deep learning techniques. *Int. Arch. Photogramm. Remote Sens. Spat. Inf. Sci.* **2022**, *XLIII-B3-2022*, 1349–1354.
86. Wang, M.; Hong, D.; Han, Z.; Li, J.; Yao, J.; Gao, L.; Zhang, B.; Chanussot, J. Tensor Decompositions for Hyperspectral Data Processing in Remote Sensing: A comprehensive review. *IEEE Geosci. Remote Sens. Mag.* **2023**, *11*, 26–72. [CrossRef]
87. Rosenfield, G.H.; Fitzpatrick-lins, K. A coefficient of agreement as a measure of thematic classification accuracy. *Photogramm. Eng. Remote Sens.* **1986**, *52*, 223–227.
88. Marsocci, V.; Coletta, V.; Ravanelli, R.; Scardapane, S.; Crespi, M. Inferring 3D change detection from bitemporal optical images. *ISPRS J. Photogramm. Remote Sens.* **2023**, *196*, 325–339. [CrossRef]

89. Galassi, A.; Lippi, M.; Torroni, P. Attention in Natural Language Processing. *IEEE Trans. Neural Netw. Learn. Syst.* **2021**, *32*, 4291–4308. [CrossRef] [PubMed]
90. Guo, M.; Xu, T.; Liu, J.; Liu, Z.; Jiang, P.; Mu, T.; Zhang, S.; Martin, R.R.; Cheng, M.; Hu, S. Attention mechanisms in computer vision: A survey. *Comput. Vis. Media* **2022**, *8*, 331–368. [CrossRef]
91. Long, J.; Shelhamer, E.; Darrell, T. Fully convolutional networks for semantic segmentation. In Proceedings of the CVPR, Boston, MA, USA, 7–12 June 2015; pp. 3431–3440.
92. Li, X.; Li, X.; Zhang, L.; Cheng, G.; Shi, J.; Lin, Z.; Tan, S.; Tong, Y. Improving semantic segmentation via decoupled body and edge supervision. In Proceedings of the ECCV 2020, Glasgow, UK, 23–28 August 2020; Springer: Berlin/Heidelberg, Germany, 2020; pp. 435–452.
93. Li, X.; He, H.; Li, X.; Li, D.; Cheng, G.; Shi, J.; Weng, L.; Tong, Y.; Lin, Z. PointFlow: Flowing Semantics Through Points for Aerial Image Segmentation. In Proceedings of the IEEE CVPR 2021, Nashville, TN, USA, 20–25 June 2021; pp. 4217–4226.
94. He, H.; Li, X.; Yang, Y.; Cheng, G.; Tong, Y.; Weng, L.; Lin, Z.; Xiang, S. Boundarysqueeze: Image segmentation as boundary squeezing. *arXiv* **2021**, arXiv:2105.11668.
95. Zhao, H.; Shi, J.; Qi, X.; Wang, X.; Jia, J. Pyramid Scene Parsing Network. In Proceedings of the CVPR 2017, Minneapolis, MN, USA, 17–22 June 2007; IEEE Computer Society: Piscataway, NJ, USA, 2017; pp. 6230–6239.
96. Chen, L.; Papandreou, G.; Schroff, F.; Adam, H. Rethinking Atrous Convolution for Semantic Image Segmentation. *arXiv* **2017**, arXiv:1706.05587.
97. Yang, W.; Yang, X.; Yan, T.; Song, H.; Xia, G. Region-Based Change Detection for Polarimetric SAR Images Using Wishart Mixture Models. *IEEE Trans. Geosci. Remote Sens.* **2016**, *54*, 6746–6756. [CrossRef]
98. Chen, P.; Li, C.; Zhang, B.; Chen, Z.; Yang, X.; Lu, K.; Zhuang, L. A Region-Based Feature Fusion Network for VHR Image Change Detection. *Remote Sens.* **2022**, *14*, 5577. [CrossRef]
99. de Carvalho, O.L.F., Jr.; de Carvalho Júnior, O.A.; de Albuquerque, A.O.; Santana, N.C.; Borges, D.L. Rethinking Panoptic Segmentation in Remote Sensing: A Hybrid Approach Using Semantic Segmentation and Non-Learning Methods. *IEEE Geosci. Remote Sens. Lett.* **2022**, *19*, 3512105. [CrossRef]
100. Atasever, U.H.; Gunen, M.A. Change Detection Approach for SAR Imagery Based on Arc-Tangential Difference Image and k-Means++. *IEEE Geosci. Remote Sens. Lett.* **2022**, *19*, 3509605. [CrossRef]
101. Yu, Q.; Zhang, M.; Yu, L.; Wang, R.; Xiao, J. SAR Image Change Detection Based on Joint Dictionary Learning With Iterative Adaptive Threshold Optimization. *IEEE J. Sel. Top. Appl. Earth Obs. Remote Sens.* **2022**, *15*, 5234–5249. [CrossRef]
102. Vinholi, J.G.; Silva, D.; Machado, R.B.; Pettersson, M.I. CNN-Based Change Detection Algorithm for Wavelength-Resolution SAR Images. *IEEE Geosci. Remote Sens. Lett.* **2022**, *19*, 4003005. [CrossRef]
103. Achanta, R.; Shaji, A.; Smith, K.; Lucchi, A.; Fua, P.; Süsstrunk, S. SLIC Superpixels Compared to State-of-the-Art Superpixel Methods. *IEEE Trans. Pattern Anal. Mach. Intell.* **2012**, *34*, 2274–2282. [CrossRef]
104. Amitrano, D.; Guida, R.; Iervolino, P. Semantic Unsupervised Change Detection of Natural Land Cover With Multitemporal Object-Based Analysis on SAR Images. *IEEE Trans. Geosci. Remote Sens.* **2021**, *59*, 5494–5514. [CrossRef]
105. Lu, J.; Li, J.; Chen, G.; Zhao, L.; Xiong, B.; Kuang, G. Improving Pixel-Based Change Detection Accuracy Using an Object Based Approach in Multitemporal SAR Flood Images. *IEEE J. Sel. Top. Appl. Earth Obs. Remote Sens.* **2015**, *8*, 3486–3496. [CrossRef]
106. Javed, A.; Jung, S.; Lee, W.H.; Han, Y. Object-Based Building Change Detection by Fusing Pixel-Level Change Detection Results Generated from Morphological Building Index. *Remote Sens.* **2020**, *12*, 2952. [CrossRef]
107. Zhang, X.; Tian, M.; Xing, Y.; Yue, Y.; Li, Y.; Yin, H.; Xia, R.; Jin, J.; Zhang, Y. ADHR-CDNet: Attentive Differential High-Resolution Change Detection Network for Remote Sensing Images. *IEEE Trans. Geosci. Remote Sens.* **2022**, *60*, 5634013. [CrossRef]
108. Han, M.; Li, R.; Zhang, C. LWCDNet: A Lightweight Fully Convolution Network for Change Detection in Optical Remote Sensing Imagery. *IEEE Geosci. Remote Sens. Lett.* **2022**, *19*, 6507905. [CrossRef]
109. Ge, C.; Ding, H.; Molina, I.; He, Y.; Peng, D. Object-Oriented Change Detection Method Based on Spectral-Spatial-Saliency Change Information and Fuzzy Integral Decision Fusion for HR Remote Sensing Images. *Remote Sens.* **2022**, *14*, 3297. [CrossRef]
110. Jiang, X.; Xiang, S.; Wang, M.; Tang, P. Dual-Pathway Change Detection Network Based on the Adaptive Fusion Module. *IEEE Geosci. Remote Sens. Lett.* **2022**, *19*, 8018905. [CrossRef]
111. Wang, L.; Wang, L.; Wang, Q.; Atkinson, P.M. SSA-SiamNet: Spatial-Wise Attention-Based Siamese Network for Hyperspectral Image Change Detection. *IEEE Trans. Geosci. Remote Sens.* **2022**, *60*, 5510018. [CrossRef]
112. Ertürk, S. Fuzzy Fusion of Change Vector Analysis and Spectral Angle Mapper for Hyperspectral Change Detection. In Proceedings of the IGARSS 2018, Valencia, Spain, 22–27 July 2018; IEEE: Piscataway, NJ, USA, 2018; pp. 5045–5048.
113. Li, H.; Gong, M.; Zhang, M.; Wu, Y. Spatially Self-Paced Convolutional Networks for Change Detection in Heterogeneous Images. *IEEE J. Sel. Top. Appl. Earth Obs. Remote Sens.* **2021**, *14*, 4966–4979. [CrossRef]
114. Wu, J.; Li, B.; Qin, Y.; Ni, W.; Zhang, H.; Fu, R.; Sun, Y. A multiscale graph convolutional network for change detection in homogeneous and heterogeneous remote sensing images. *Int. J. Appl. Earth Obs. Geoinf.* **2021**, *105*, 102615. [CrossRef]
115. Wan, L.; Xiang, Y.; You, H. An Object-Based Hierarchical Compound Classification Method for Change Detection in Heterogeneous Optical and SAR Images. *IEEE Trans. Geosci. Remote Sens.* **2019**, *57*, 9941–9959. [CrossRef]
116. Wang, J.; Dobigeon, N.; Chabert, M.; Wang, D.; Huang, J.; Huang, T. CD-GAN: A robust fusion-based generative adversarial network for unsupervised change detection between heterogeneous images. *arXiv* **2022**, arXiv:2203.00948.

117. Marmol, U.; Borowiec, N. Analysis and Verification of Building Changes Based on Point Clouds from Different Sources and Time Periods. *Remote Sens.* **2023**, *15*, 1414. [CrossRef]
118. Chai, J.X.; Zhang, Y.S.; Yang, Z.; Wu, J. 3D change detection of point clouds based on density adaptive local euclidean distance. *Int. Arch. Photogramm. Remote Sens. Spat. Inf. Sci.* **2022**, *XLIII-B2-2022*, 523–530.
119. Marinelli, D.; Paris, C.; Bruzzone, L. A Novel Approach to 3-D Change Detection in Multitemporal LiDAR Data Acquired in Forest Areas. *IEEE Trans. Geosci. Remote Sens.* **2018**, *56*, 3030–3046. [CrossRef]
120. Bu, S.; Li, Q.; Han, P.; Leng, P.; Li, K. Mask-CDNet: A mask based pixel change detection network. *Neurocomputing* **2020**, *378*, 166–178. [CrossRef]
121. Gong, M.; Zhan, T.; Zhang, P.; Miao, Q. Superpixel-Based Difference Representation Learning for Change Detection in Multispectral Remote Sensing Images. *IEEE Trans. Geosci. Remote Sens.* **2017**, *55*, 2658–2673. [CrossRef]
122. Zhang, X.; Liu, G.; Zhang, C.; Atkinson, P.M.; Tan, X.; Jian, X.; Zhou, X.; Li, Y. Two-Phase Object-Based Deep Learning for Multi-Temporal SAR Image Change Detection. *Remote Sens.* **2020**, *12*, 548. [CrossRef]
123. Zhang, W.; Jiao, L.; Liu, F.; Yang, S.; Song, W.; Liu, J. Sparse Feature Clustering Network for Unsupervised SAR Image Change Detection. *IEEE Trans. Geosci. Remote Sens.* **2022**, *60*, 5226713. [CrossRef]
124. Saha, S.; Bovolo, F.; Bruzzone, L. Building Change Detection in VHR SAR Images via Unsupervised Deep Transcoding. *IEEE Trans. Geosci. Remote Sens.* **2021**, *59*, 1917–1929. [CrossRef]
125. Wang, C.; Su, W.; Gu, H. SAR Image Change Detection Based on Semisupervised Learning and Two-Step Training. *IEEE Geosci. Remote Sens. Lett.* **2022**, *19*, 4008905. [CrossRef]
126. Wang, J.; Wang, Y.; Chen, B.; Liu, H. LCS-EnsemNet: A Semisupervised Deep Neural Network for SAR Image Change Detection with Dual Feature Extraction and Label-Consistent Self-Ensemble. *IEEE J. Sel. Top. Appl. Earth Obs. Remote Sens.* **2021**, *14*, 11903–11925. [CrossRef]
127. Chen, G.; Zhao, Y.; Wang, Y.; Yap, K. SSN: Stockwell Scattering Network for SAR Image Change Detection. *IEEE Geosci. Remote Sens. Lett.* **2023**, *20*, 4001405. [CrossRef]
128. Zhang, X.; Su, X.; Yuan, Q.; Wang, Q. Spatial-Temporal Gray-Level Co-Occurrence Aware CNN for SAR Image Change Detection. *IEEE Geosci. Remote Sens. Lett.* **2022**, *19*, 4018605. [CrossRef]
129. Bergamasco, L.; Saha, S.; Bovolo, F.; Bruzzone, L. Unsupervised Change Detection Using Convolutional-Autoencoder Multiresolution Features. *IEEE Trans. Geosci. Remote Sens.* **2022**, *60*, 4408119. [CrossRef]
130. Chen, Y.; Bruzzone, L. A Self-Supervised Approach to Pixel-Level Change Detection in Bi-Temporal RS Images. *IEEE Trans. Geosci. Remote Sens.* **2022**, *60*, 4413911. [CrossRef]
131. Shi, J.; Wu, T.; Qin, A.K.; Lei, Y.; Jeon, G. Semisupervised Adaptive Ladder Network for Remote Sensing Image Change Detection. *IEEE Trans. Geosci. Remote Sens.* **2022**, *60*, 5408220. [CrossRef]
132. Wang, J.X.; Li, T.; Chen, S.B.; Tang, J.; Luo, B.; Wilson, R.C. Reliable Contrastive Learning for Semi-Supervised Change Detection in Remote Sensing Images. *IEEE Trans. Geosci. Remote. Sens.* **2022**, *60*, 4416413. [CrossRef]
133. Zhang, X.; Yue, Y.; Gao, W.; Yun, S.; Su, Q.; Yin, H.; Zhang, Y. DifUnet++: A Satellite Images Change Detection Network Based on Unet++ and Differential Pyramid. *IEEE Geosci. Remote Sens. Lett.* **2022**, *19*, 8006605. [CrossRef]
134. Li, X.; Yan, L.; Zhang, Y.; Mo, N. SDMNet: A Deep-Supervised Dual Discriminative Metric Network for Change Detection in High-Resolution Remote Sensing Images. *IEEE Geosci. Remote Sens. Lett.* **2022**, *19*, 5513905. [CrossRef]
135. Li, Q.; Gong, H.; Dai, H.; Li, C.; He, Z.; Wang, W.; Feng, Y.; Han, F.; Tuniyazi, A.; Li, H.; et al. Unsupervised Hyperspectral Image Change Detection via Deep Learning Self-Generated Credible Labels. *IEEE J. Sel. Top. Appl. Earth Obs. Remote Sens.* **2021**, *14*, 9012–9024. [CrossRef]
136. Hu, M.; Wu, C.; Du, B.; Zhang, L. Binary Change Guided Hyperspectral Multiclass Change Detection. *IEEE Trans. Image Process.* **2023**, *32*, 791–806. [CrossRef]
137. Liu, S.; Tong, X.; Bruzzone, L.; Du, P. A novel semisupervised framework for multiple change detection in hyperspectral images. In Proceedings of the 2017 IEEE International Geoscience and Remote Sensing Symposium, IGARSS 2017, Fort Worth, TX, USA, 23–28 July 2017; IEEE: Piscataway, NJ, USA, 2017; pp. 173–176.
138. Wang, L.; Wang, L.; Wang, Q.; Bruzzone, L. RSCNet: A Residual Self-Calibrated Network for Hyperspectral Image Change Detection. *IEEE Trans. Geosci. Remote Sens.* **2022**, *60*, 5529917. [CrossRef]
139. Shi, C.; Zhang, Z.; Zhang, W.; Zhang, C.; Xu, Q. Learning Multiscale Temporal-Spatial-Spectral Features via a Multipath Convolutional LSTM Neural Network for Change Detection with Hyperspectral Images. *IEEE Trans. Geosci. Remote Sens.* **2022**, *60*, 5529816. [CrossRef]
140. Jia, M.; Zhang, C.; Lv, Z.; Zhao, Z.; Wang, L. Bipartite Adversarial Autoencoders with Structural Self-Similarity for Unsupervised Heterogeneous Remote Sensing Image Change Detection. *IEEE Geosci. Remote Sens. Lett.* **2022**, *19*, 6515705. [CrossRef]
141. Luppino, L.T.; Kampffmeyer, M.; Bianchi, F.M.; Moser, G.; Serpico, S.B.; Jenssen, R.; Anfinsen, S.N. Deep Image Translation with an Affinity-Based Change Prior for Unsupervised Multimodal Change Detection. *IEEE Trans. Geosci. Remote Sens.* **2022**, *60*, 4700422. [CrossRef]
142. Jiang, X.; Li, G.; Zhang, X.; He, Y. A Semisupervised Siamese Network for Efficient Change Detection in Heterogeneous Remote Sensing Images. *IEEE Trans. Geosci. Remote Sens.* **2022**, *60*, 4700718. [CrossRef]
143. Jiang, X.; Li, G.; Liu, Y.; Zhang, X.S.; He, Y. Change Detection in Heterogeneous Optical and SAR Remote Sensing Images Via Deep Homogeneous Feature Fusion. *IEEE J. Sel. Top. Appl. Earth Obs. Remote Sens.* **2020**, *13*, 1551–1566. [CrossRef]

144. Xiao, W.; Xu, S.; Elberink, S.O.; Vosselman, G. Individual Tree Crown Modeling and Change Detection From Airborne Lidar Data. *IEEE J. Sel. Top. Appl. Earth Obs. Remote Sens.* **2016**, *9*, 3467–3477. [CrossRef]
145. Marinelli, D.; Coops, N.C.; Bolton, D.K.; Bruzzone, L. Forest Change Detection in Lidar Data Based on Polar Change Vector Analysis. *IEEE Geosci. Remote Sens. Lett.* **2022**, *19*, 6500105. [CrossRef]
146. Yadav, R.; Nascetti, A.; Ban, Y. Building Change Detection using Multi-Temporal Airborne LiDAR Data. *arXiv* **2022**, arXiv:2204.12535.
147. de Gélis, I.; Lefèvre, S.; Corpetti, T. Siamese KPConv: 3D multiple change detection from raw point clouds using deep learning. *ISPRS J. Photogramm. Remote Sens.* **2023**, *197*, 274–291. [CrossRef]
148. Peng, D.; Zhang, Y.; Guan, H. End-to-End Change Detection for High Resolution Satellite Images Using Improved UNet++. *Remote Sens.* **2019**, *11*, 1382. [CrossRef]
149. Dong, H.; Ma, W.; Jiao, L.; Liu, F.; Li, L. A Multiscale Self-Attention Deep Clustering for Change Detection in SAR Images. *IEEE Trans. Geosci. Remote Sens.* **2022**, *60*, 5207016. [CrossRef]
150. Li, X.; Gao, F.; Dong, J.; Qi, L. Change Detection in Sar Images Based on A Multi-Scale Attention Convolution Network. In Proceedings of the IGARSS 2022, Kuala Lumpur, Malaysia, 17–22 July 2022; IEEE: Piscataway, NJ, USA, 2022; pp. 3219–3222.
151. Zhao, C.; Ma, L.; Wang, L.; Ohtsuki, T.; Mathiopoulos, P.T.; Wang, Y. SAR Image Change Detection in Spatial-Frequency Domain Based on Attention Mechanism and Gated Linear Unit. *IEEE Geosci. Remote Sens. Lett.* **2023**, *20*, 4002205. [CrossRef]
152. Yan, T.; Wan, Z.; Zhang, P.; Cheng, G.; Lu, H. TransY-Net: Learning Fully Transformer Networks for Change Detection of Remote Sensing Images. *IEEE Trans. Geosci. Remote Sens.* **2023**, *61*, 4410012. [CrossRef]
153. Yan, L.; Jiang, J. A Hybrid Siamese Network with Spatiotemporal Enhancement and Two-Level Feature Fusion for Remote Sensing Image Change Detection. *IEEE Trans. Geosci. Remote Sens.* **2023**, *61*, 4403217. [CrossRef]
154. Chen, K.; Chen, B.; Liu, C.; Li, W.; Zou, Z.; Shi, Z. RSMamba: Remote Sensing Image Classification with State Space Model. *arXiv* **2024**, arXiv:2403.19654.
155. Wang, G.; Zhang, X.; Peng, Z.; Zhang, T.; Jia, X.; Jiao, L. S^2Mamba: A Spatial-spectral State Space Model for Hyperspectral Image Classification. *arXiv* **2024**, arXiv:2404.18213.
156. Zhao, S.; Chen, H.; Zhang, X.; Xiao, P.; Bai, L.; Ouyang, W. Rs-mamba for large remote sensing image dense prediction. *arXiv* **2024**, arXiv:2404.02668.
157. Liu, C.; Chen, K.; Chen, B.; Zhang, H.; Zou, Z.; Shi, Z. RSCaMa: Remote Sensing Image Change Captioning with State Space Model. *arXiv* **2024**, arXiv:2404.18895.
158. Yu, X.; Yue, X. Similarity Matrix Entropy for Multitemporal Polarimetric SAR Change Detection. *IEEE Geosci. Remote Sens. Lett.* **2022**, *19*, 4003805. [CrossRef]
159. Liu, Z.; Chen, Z.; Li, L. An Automatic High Confidence Sets Selection Strategy for SAR Images Change Detection. *IEEE Geosci. Remote Sens. Lett.* **2022**, *19*, 4003505. [CrossRef]
160. Vinholi, J.G.; Palm, B.G.; Silva, D.; Machado, R.B.; Pettersson, M.I. Change Detection Based on Convolutional Neural Networks Using Stacks of Wavelength-Resolution Synthetic Aperture Radar Images. *IEEE Trans. Geosci. Remote Sens.* **2022**, *60*, 5236414. [CrossRef]
161. Qu, X.; Gao, F.; Dong, J.; Du, Q.; Li, H. Change Detection in Synthetic Aperture Radar Images Using a Dual-Domain Network. *IEEE Geosci. Remote Sens. Lett.* **2022**, *19*, 4013405. [CrossRef]
162. Shao, P.; Yi, Y.; Liu, Z.; Dong, T.; Ren, D. Novel Multiscale Decision Fusion Approach to Unsupervised Change Detection for High-Resolution Images. *IEEE Geosci. Remote Sens. Lett.* **2022**, *19*, 2503105. [CrossRef]
163. Fang, H.; Du, P.; Wang, X.; Lin, C.; Tang, P. Unsupervised Change Detection Based on Weighted Change Vector Analysis and Improved Markov Random Field for High Spatial Resolution Imagery. *IEEE Geosci. Remote Sens. Lett.* **2022**, *19*, 1. [CrossRef]
164. Zhu, S.; Song, Y.; Zhang, Y.; Zhang, Y. ECFNet: A Siamese Network with Fewer FPs and Fewer FNs for Change Detection of Remote-Sensing Images. *IEEE Geosci. Remote Sens. Lett.* **2023**, *20*, 6001005. [CrossRef]
165. Chen, H.; Li, W.; Chen, S.; Shi, Z. Semantic-Aware Dense Representation Learning for Remote Sensing Image Change Detection. *IEEE Trans. Geosci. Remote Sens.* **2022**, *60*, 5630018. [CrossRef]
166. Song, X.; Hua, Z.; Li, J. Remote Sensing Image Change Detection Transformer Network Based on Dual-Feature Mixed Attention. *IEEE Trans. Geosci. Remote Sens.* **2022**, *60*, 5920416. [CrossRef]
167. Liu, M.; Shi, Q.; Chai, Z.; Li, J. PA-Former: Learning Prior-Aware Transformer for Remote Sensing Building Change Detection. *IEEE Geosci. Remote Sens. Lett.* **2022**, *19*, 6515305. [CrossRef]
168. Zhang, X.; Cheng, S.; Wang, L.; Li, H. Asymmetric Cross-Attention Hierarchical Network Based on CNN and Transformer for Bitemporal Remote Sensing Images Change Detection. *IEEE Trans. Geosci. Remote Sens.* **2023**, *61*, 2000415. [CrossRef]
169. Hu, M.; Wu, C.; Zhang, L.; Du, B. Hyperspectral Anomaly Change Detection Based on Autoencoder. *IEEE J. Sel. Top. Appl. Earth Obs. Remote Sens.* **2021**, *14*, 3750–3762. [CrossRef]
170. Chang, S.; Kopp, M.; Ghamisi, P. Sketched Multiview Subspace Learning for Hyperspectral Anomalous Change Detection. *IEEE Trans. Geosci. Remote Sens.* **2022**, *60*, 5543412. [CrossRef]
171. Ge, H.; Tang, Y.; Bi, Z.; Zhan, T.; Xu, Y.; Song, A. MMSRC: A Multidirection Multiscale Spectral-Spatial Residual Network for Hyperspectral Multiclass Change Detection. *IEEE J. Sel. Top. Appl. Earth Obs. Remote Sens.* **2022**, *15*, 9254–9265. [CrossRef]
172. Ou, X.; Liu, L.; Tu, B.; Zhang, G.; Xu, Z. A CNN Framework with Slow-Fast Band Selection and Feature Fusion Grouping for Hyperspectral Image Change Detection. *IEEE Trans. Geosci. Remote Sens.* **2022**, *60*, 5524716. [CrossRef]

173. Wang, Y.; Hong, D.; Sha, J.; Gao, L.; Liu, L.; Zhang, Y.; Rong, X. Spectral-Spatial-Temporal Transformers for Hyperspectral Image Change Detection. *IEEE Trans. Geosci. Remote Sens.* **2022**, *60*, 5536814. [CrossRef]
174. Dong, W.; Zhao, J.; Qu, J.; Xiao, S.; Li, N.; Hou, S.; Li, Y. Abundance Matrix Correlation Analysis Network Based on Hierarchical Multihead Self-Cross-Hybrid Attention for Hyperspectral Change Detection. *IEEE Trans. Geosci. Remote Sens.* **2023**, *61*, 5501513. [CrossRef]
175. Song, R.; Ni, W.; Cheng, W.; Wang, X. CSANet: Cross-Temporal Interaction Symmetric Attention Network for Hyperspectral Image Change Detection. *IEEE Geosci. Remote Sens. Lett.* **2022**, *19*, 6010105. [CrossRef]
176. Yang, Y.; Qu, J.; Xiao, S.; Dong, W.; Li, Y.; Du, Q. A Deep Multiscale Pyramid Network Enhanced with Spatial-Spectral Residual Attention for Hyperspectral Image Change Detection. *IEEE Trans. Geosci. Remote Sens.* **2022**, *60*, 5525513. [CrossRef]
177. Sun, Y.; Lei, L.; Guan, D.; Kuang, G.; Liu, L. Graph Signal Processing for Heterogeneous Change Detection. *IEEE Trans. Geosci. Remote Sens.* **2022**, *60*, 4415823. [CrossRef]
178. Sun, Y.; Lei, L.; Guan, D.; Li, M.; Kuang, G. Sparse-Constrained Adaptive Structure Consistency-Based Unsupervised Image Regression for Heterogeneous Remote-Sensing Change Detection. *IEEE Trans. Geosci. Remote Sens.* **2022**, *60*, 4405814. [CrossRef]
179. Wu, Y.; Li, J.; Yuan, Y.; Qin, A.K.; Miao, Q.; Gong, M. Commonality Autoencoder: Learning Common Features for Change Detection From Heterogeneous Images. *IEEE Trans. Neural Netw. Learn. Syst.* **2022**, *33*, 4257–4270. [CrossRef]
180. Hu, L.; Liu, J.; Xiao, L. A Total Variation Regularized Bipartite Network for Unsupervised Change Detection. *IEEE Trans. Geosci. Remote Sens.* **2022**, *60*, 1–18. [CrossRef]
181. Zhang, C.; Feng, Y.; Hu, L.; Tapete, D.; Pan, L.; Liang, Z.; Cigna, F.; Yue, P. A domain adaptation neural network for change detection with heterogeneous optical and SAR remote sensing images. *Int. J. Appl. Earth Obs. Geoinf.* **2022**, *109*, 102769. [CrossRef]
182. Wang, X.; Cheng, W.; Feng, Y.; Song, R. TSCNet: Topological Structure Coupling Network for Change Detection of Heterogeneous Remote Sensing Images. *Remote Sens.* **2023**, *15*, 621. [CrossRef]
183. Dai, C.; Zhang, Z.; Lin, D. An Object-Based Bidirectional Method for Integrated Building Extraction and Change Detection between Multimodal Point Clouds. *Remote Sens.* **2020**, *12*, 1680. [CrossRef]
184. Liu, D.; Li, D.; Wang, M.; Wang, Z. 3D Change Detection Using Adaptive Thresholds Based on Local Point Cloud Density. *ISPRS Int. J. Geo Inf.* **2021**, *10*, 127. [CrossRef]
185. Nagy, B.; Kovács, L.; Benedek, C. ChangeGAN: A Deep Network for Change Detection in Coarsely Registered Point Clouds. *IEEE Robot. Autom. Lett.* **2021**, *6*, 8277–8284. [CrossRef]
186. Zhang, C.; Wang, L.; Cheng, S.; Li, Y. SwinSUNet: Pure Transformer Network for Remote Sensing Image Change Detection. *IEEE Trans. Geosci. Remote Sens.* **2022**, *60*, 5224713. [CrossRef]
187. Liu, R.; Wang, R.; Huang, J.; Li, J.; Jiao, L. Change Detection in SAR Images Using Multiobjective Optimization and Ensemble Strategy. *IEEE Geosci. Remote Sens. Lett.* **2021**, *18*, 1585–1589. [CrossRef]
188. Fang, W.; Xi, C. Land-Cover Change Detection for SAR Images Based on Biobjective Fuzzy Local Information Clustering Method with Decomposition. *IEEE Geosci. Remote Sens. Lett.* **2022**, *19*, 4506105. [CrossRef]
189. Gong, M.; Zhou, Z.; Ma, J. Change Detection in Synthetic Aperture Radar Images based on Image Fusion and Fuzzy Clustering. *IEEE Trans. Image Process.* **2012**, *21*, 2141–2151. [CrossRef] [PubMed]
190. Gao, F.; Dong, J.; Li, B.; Xu, Q. Automatic Change Detection in Synthetic Aperture Radar Images Based on PCANet. *IEEE Geosci. Remote Sens. Lett.* **2016**, *13*, 1792–1796. [CrossRef]
191. Gao, Y.; Gao, F.; Dong, J.; Wang, S. Change Detection From Synthetic Aperture Radar Images Based on Channel Weighting-Based Deep Cascade Network. *IEEE J. Sel. Top. Appl. Earth Obs. Remote Sens.* **2019**, *12*, 4517–4529. [CrossRef]
192. Wang, R.; Ding, F.; Chen, J.; Liu, B.; Zhang, J.; Jiao, L. SAR Image Change Detection Method via a Pyramid Pooling Convolutional Neural Network. In Proceedings of the IGARSS 2020, Waikoloa, HI, USA, 26 September–2 October 2020; IEEE: Piscataway, NJ, USA, 2020; pp. 312–315.
193. Jiang, Y.; Hu, L.; Zhang, Y.; Yang, X. WRICNet: A Weighted Rich-scale Inception Coder Network for Multi-Resolution Remote Sensing Image Change Detection. *arXiv* **2021**, arXiv:2108.07955.
194. Lin, M.; Yang, G.; Zhang, H. Transition Is a Process: Pair-to-Video Change Detection Networks for Very High Resolution Remote Sensing Images. *IEEE Trans. Image Process.* **2023**, *32*, 57–71. [CrossRef] [PubMed]
195. Zhao, M.; Zhao, Z.; Gong, S.; Liu, Y.; Yang, J.; Xiong, X.; Li, S. Spatially and Semantically Enhanced Siamese Network for Semantic Change Detection in High-Resolution Remote Sensing Images. *IEEE J. Sel. Top. Appl. Earth Obs. Remote Sens.* **2022**, *15*, 2563–2573. [CrossRef]
196. Caye Daudt, R.; Le Saux, B.; Boulch, A. Fully Convolutional Siamese Networks for Change Detection. In Proceedings of the 2018 25th IEEE International Conference on Image Processing (ICIP), Athens, Greece, 7–10 October 2018; pp. 4063–4067.
197. Fang, S.; Li, K.; Shao, J.; Li, Z. SNUNet-CD: A Densely Connected Siamese Network for Change Detection of VHR Images. *IEEE Geosci. Remote Sens. Lett.* **2022**, *19*, 8007805. [CrossRef]
198. Han, C.; Wu, C.; Guo, H.; Hu, M.; Li, J.; Chen, H. Change Guiding Network: Incorporating Change Prior to Guide Change Detection in Remote Sensing Imagery. *IEEE J. Sel. Top. Appl. Earth Obs. Remote Sens.* **2023**, *16*, 8395–8407. [CrossRef]
199. Bandara, W.G.C.; Patel, V.M. A Transformer-Based Siamese Network for Change Detection. In Proceedings of the IGARSS 2022—2022 IEEE International Geoscience and Remote Sensing Symposium, Kuala Lumpur, Malaysia, 17–22 July 2022; pp. 207–210.

200. Zhang, H.; Lin, M.; Yang, G.; Zhang, L. ESCNet: An End-to-End Superpixel-Enhanced Change Detection Network for Very-High-Resolution Remote Sensing Images. *IEEE Trans. Neural Netw. Learn. Syst.* **2023**, *34*, 28–42. [CrossRef]
201. Daudt, R.C.; Saux, B.L.; Boulch, A.; Gousseau, Y. Multitask learning for large-scale semantic change detection. *Comput. Vis. Image Underst.* **2019**, *187*, 102783. [CrossRef]
202. Cui, F.; Jiang, J. MTSCD-Net: A network based on multi-task learning for semantic change detection of bitemporal remote sensing images. *Int. J. Appl. Earth Obs. Geoinf.* **2023**, *118*, 103294. [CrossRef]
203. Ding, L.; Zhang, J.; Zhang, K.; Guo, H.; Liu, B.; Bruzzone, L. Joint Spatio-Temporal Modeling for the Semantic Change Detection in Remote Sensing Images. *IEEE Trans. Geosci. Remote Sens.* **2024**, *62*, 5610814. [CrossRef]
204. Celik, T. Unsupervised Change Detection in Satellite Images Using Principal Component Analysis and *k*-Means Clustering. *IEEE Geosci. Remote Sens. Lett.* **2009**, *6*, 772–776. [CrossRef]
205. Zhang, H.; Gong, M.; Zhang, P.; Su, L.; Shi, J. Feature-Level Change Detection Using Deep Representation and Feature Change Analysis for Multispectral Imagery. *IEEE Geosci. Remote Sens. Lett.* **2016**, *13*, 1666–1670. [CrossRef]
206. Chen, H.; Wu, C.; Du, B.; Zhang, L.; Wang, L. Change Detection in Multisource VHR Images via Deep Siamese Convolutional Multiple-Layers Recurrent Neural Network. *IEEE Trans. Geosci. Remote Sens.* **2020**, *58*, 2848–2864. [CrossRef]
207. Yang, M.; Jiao, L.; Liu, F.; Hou, B.; Yang, S.; Jian, M. DPFL-Nets: Deep Pyramid Feature Learning Networks for Multiscale Change Detection. *IEEE Trans. Neural Netw. Learn. Syst.* **2022**, *33*, 6402–6416. [CrossRef]
208. Luppino, L.T.; Bianchi, F.M.; Moser, G.; Anfinsen, S.N. Unsupervised Image Regression for Heterogeneous Change Detection. *IEEE Trans. Geosci. Remote Sens.* **2019**, *57*, 9960–9975. [CrossRef]
209. Niu, X.; Gong, M.; Zhan, T.; Yang, Y. A Conditional Adversarial Network for Change Detection in Heterogeneous Images. *IEEE Geosci. Remote Sens. Lett.* **2019**, *16*, 45–49. [CrossRef]
210. Mou, L.; Zhu, X. IM2HEIGHT: Height Estimation from Single Monocular Imagery via Fully Residual Convolutional-Deconvolutional Network. *arXiv* **2018**, arXiv:1802.10249.
211. Zhou, Q.; Feng, Z.; Gu, Q.; Pang, J.; Cheng, G.; Lu, X.; Shi, J.; Ma, L. Context-aware mixup for domain adaptive semantic segmentation. *IEEE Trans. Circuits Syst. Video Technol.* **2022**, *33*, 804–817. [CrossRef]
212. Catalano, N.; Matteucci, M. Few Shot Semantic Segmentation: A review of methodologies and open challenges. *arXiv* **2023**, arXiv:2304.05832.
213. Han, Y.; Zhang, J.; Xue, Z.; Xu, C.; Shen, X.; Wang, Y.; Wang, C.; Liu, Y.; Li, X. Reference Twice: A Simple and Unified Baseline for Few-Shot Instance Segmentation. *arXiv* **2023**, arXiv:2301.01156.
214. Zhou, K.; Liu, Z.; Qiao, Y.; Xiang, T.; Loy, C.C. Domain generalization: A survey. *IEEE Trans. Pattern Anal. Mach. Intell.* **2022**, *45*, 4396–4415. [CrossRef]
215. Carion, N.; Massa, F.; Synnaeve, G.; Usunier, N.; Kirillov, A.; Zagoruyko, S. End-to-end object detection with transformers. In Proceedings of the Computer Vision—ECCV 2020: 16th European Conference, Glasgow, UK, 23–28 August 2020; Part I 16; Springer: Berlin/Heidelberg, Germany, 2020; pp. 213–229.
216. Xu, S.; Li, X.; Wang, J.; Cheng, G.; Tong, Y.; Tao, D. Fashionformer: A simple, effective and unified baseline for human fashion segmentation and recognition. In Proceedings of the Computer Vision—ECCV 2022: 17th European Conference, Tel Aviv, Israel, 23–27 October 2022; Part XXXVII; Springer: Berlin/Heidelberg, Germany, 2022; pp. 545–563.
217. Li, X.; Xu, S.; Yang, Y.; Yuan, H.; Cheng, G.; Tong, Y.; Lin, Z.; Tao, D. PanopticPartFormer++: A Unified and Decoupled View for Panoptic Part Segmentation. *arXiv* **2023**, arXiv:2301.00954.
218. Li, X.; Yuan, H.; Zhang, W.; Cheng, G.; Pang, J.; Loy, C.C. Tube-Link: A Flexible Cross Tube Baseline for Universal Video Segmentation. *arXiv* **2023**, arXiv:2303.12782.
219. Lv, W.; Xu, S.; Zhao, Y.; Wang, G.; Wei, J.; Cui, C.; Du, Y.; Dang, Q.; Liu, Y. DETRs Beat YOLOs on Real-time Object Detection. *arXiv* **2023**, arXiv:2304.08069.
220. Li, X.; Zhang, W.; Pang, J.; Chen, K.; Cheng, G.; Tong, Y.; Loy, C.C. Video k-net: A simple, strong, and unified baseline for video segmentation. In Proceedings of the IEEE/CVF Conference on Computer Vision and Pattern Recognition, New Orleans, LA, USA, 21–24 June 2022; pp. 18847–18857.
221. Li, D.; Hu, J.; Wang, C.; Li, X.; She, Q.; Zhu, L.; Zhang, T.; Chen, Q. Involution: Inverting the Inherence of Convolution for Visual Recognition. In Proceedings of the IEEE/CVF Conference on Computer Vision and Pattern Recognition (CVPR), Nashville, TN, USA, 20–25 June 2021; pp. 12321–12330.
222. Wang, Y.; Yang, Y.; Li, Z.; Bai, J.; Zhang, M.; Li, X.; Yu, J.; Zhang, C.; Huang, G.; Tong, Y. Convolution-enhanced Evolving Attention Networks. *IEEE Trans. Pattern Anal. Mach. Intell.* **2023**, *45*, 8176–8192. [CrossRef] [PubMed]
223. Douillard, A.; Chen, Y.; Dapogny, A.; Cord, M. PLOP: Learning Without Forgetting for Continual Semantic Segmentation. In Proceedings of the CVPR 2021, Nashville, TN, USA, 20–25 June 2021; pp. 4040–4050.
224. Feng, Y.; Sun, X.; Diao, W.; Li, J.; Gao, X.; Fu, K. Continual Learning with Structured Inheritance for Semantic Segmentation in Aerial Imagery. *IEEE Trans. Geosci. Remote Sens.* **2022**, *60*, 1–17. [CrossRef]
225. Li, X.; You, A.; Zhu, Z.; Zhao, H.; Yang, M.; Yang, K.; Tan, S.; Tong, Y. Semantic flow for fast and accurate scene parsing. In Proceedings of the Computer Vision—ECCV 2020: 16th European Conference, Glasgow, UK, 23–28 August 2020; Part I 16; Springer: Berlin/Heidelberg, Germany, 2020; pp. 775–793.
226. Zhang, J.; Li, X.; Li, J.; Liu, L.; Xue, Z.; Zhang, B.; Jiang, Z.; Huang, T.; Wang, Y.; Wang, C. Rethinking Mobile Block for Efficient Neural Models. *arXiv* **2023**, arXiv:2301.01146.

227. Li, X.; Li, X.; You, A.; Zhang, L.; Cheng, G.; Yang, K.; Tong, Y.; Lin, Z. Towards Efficient Scene Understanding via Squeeze Reasoning. *IEEE Trans. Image Process.* **2021**, *30*, 7050–7063. [CrossRef]
228. Wan, Q.; Huang, Z.; Lu, J.; Yu, G.; Zhang, L. Seaformer: Squeeze-enhanced axial transformer for mobile semantic segmentation. In Proceedings of the ICLR 2023, Kigali, Rwanda, 1–5 May 2023.
229. Liu, Y.; Chu, L.; Chen, G.; Wu, Z.; Chen, Z.; Lai, B.; Hao, Y. PaddleSeg: A High-Efficient Development Toolkit for Image Segmentation. *arXiv* **2021**, arXiv:2101.06175.
230. Chen, J.; Wang, S.; Chen, L.; Cai, H.; Qian, Y. Incremental Detection of Remote Sensing Objects with Feature Pyramid and Knowledge Distillation. *IEEE Trans. Geosci. Remote Sens.* **2022**, *60*, 5600413. [CrossRef]
231. Zhang, Y.; Yan, Z.; Sun, X.; Diao, W.; Fu, K.; Wang, L. Learning Efficient and Accurate Detectors with Dynamic Knowledge Distillation in Remote Sensing Imagery. *IEEE Trans. Geosci. Remote Sens.* **2022**, *60*, 5613819. [CrossRef]
232. Wu, W.; Zhao, Y.; Shou, M.Z.; Zhou, H.; Shen, C. DiffuMask: Synthesizing Images with Pixel-level Annotations for Semantic Segmentation Using Diffusion Models. *arXiv* **2023**, arXiv:2303.11681.
233. Bandara, W.G.C.; Nair, N.G.; Patel, V.M. DDPM-CD: Remote Sensing Change Detection using Denoising Diffusion Probabilistic Models. *arXiv* **2022**, arXiv:2206.11892.
234. Wen, Y.; Zhang, Z.; Cao, Q.; Niu, G. TransC-GD-CD: Transformer-Based Conditional Generative Diffusion Change Detection Model. *IEEE J. Sel. Top. Appl. Earth Obs. Remote Sens.* **2024**, *17*, 7144–7158. [CrossRef]
235. Cai, L.; Zhang, Z.; Zhu, Y.; Zhang, L.; Li, M.; Xue, X. Bigdetection: A large-scale benchmark for improved object detector pre-training. In Proceedings of the CVPR, New Orleans, LA, USA, 21–24 June 2022; pp. 4777–4787.
236. Zhao, Q.; Lyu, S.; Chen, L.; Liu, B.; Xu, T.B.; Cheng, G.; Feng, W. Learn by Oneself: Exploiting Weight-Sharing Potential in Knowledge Distillation Guided Ensemble Network. *IEEE Trans. Circuits Syst. Video Technol.* **2023**, *33*, 6661–6678. [CrossRef]
237. Kirillov, A.; Mintun, E.; Ravi, N.; Mao, H.; Rolland, C.; Gustafson, L.; Xiao, T.; Whitehead, S.; Berg, A.C.; Lo, W.Y.; et al. Segment Anything. *arXiv* **2023**, arXiv:2304.02643.
238. Wang, X.; Wang, W.; Cao, Y.; Shen, C.; Huang, T. Images Speak in Images: A Generalist Painter for In-Context Visual Learning. In Proceedings of the 2023 IEEE/CVF Conference on Computer Vision and Pattern Recognition (CVPR), Vancouver, BC, Canada, 17–24 June 2023.
239. Wang, X.; Zhang, X.; Cao, Y.; Wang, W.; Shen, C.; Huang, T. SegGPT: Segmenting Everything In Context. *arXiv* **2023**, arXiv:2304.03284.